ARTHROPOD SYSTEMATICS & PHYLOGENY

76 (2): 303–322
18.7.2018

SENCKENBERG

Eureka: discovery of male *Turgiditarsus* Schillhammer reveals its placement in Acylophorina and resolves phylogenetic relationships within the subtribe (Coleoptera: Staphylinidae: Staphylininae)

Harald Schillhammer[1] & Adam J. Brunke*,[2]

[1] Natural History Museum of Vienna, Entomology Department, Burgring 7, A-1014, Vienna, Austria; Harald Schillhammer [harald.schillhammer@nhm-wien.ac.at] — [2] Canadian National Collection of Insects, Arachnids and Nematodes, Agriculture and Agri-Food Canada, 960 Carling Avenue, K.W. Neatby Building, Ottawa, Ontario, Canada, K1A 0C6; Adam Brunke * [adam.j.brunke@gmail.com] — * Corresponding author

Accepted 28.iii.2018.
Published online at www.senckenberg.de/arthropod-systematics on 29.vi.2018.
Editors in charge: Monika J.B. Eberhard & Klaus-Dieter Klass

Abstract. *Turgiditarsus* Schillhammer comprises some of the most bizarre and rarely encountered rove beetles in the subfamily Staphylininae. The genus is presently known from only 4 female specimens comprising three species in the eastern Oriental region. Its previous placement in Anisolinina was based primarily on superficial similarity, much before recent advances in the systematics of tribe Staphylinini. Total evidence phylogenetic analysis of a broad taxon sample within Staphylinini, including the first male specimen of *Turgiditarsus*, revealed that the genus should be placed in the morphologically diverse and relictual Acylophorina, a subtribe with one of the oldest crown group ages in the latest Early Cretaceous. *Turgiditarsus* is redescribed and two new species, *T. eureka* Schillhammer and Brunke **sp.n.** and *T. vietnamensis* Schillhammer and Brunke **sp.n.**, are described, bringing the total number to five. *Amacylophorus* Smetana **stat.n.**, a subgenus of *Acylophorus* Gravenhorst, is raised to genus rank and redescribed, with the following new combination: *Amacylophorus pratensis* (LeConte) **comb.n.** *Stevensia* Cameron and its single species, recently moved to this subtribe, are redescribed. All genera of Acylophorina are diagnosed and included in a novel world key. A species level key is updated for *Turgiditarsus*. Further systematic work within diverse *Acylophorus* is needed to re-assess the status of *Acylohsellus*, *Paratolmerus* and the remaining subgenera of *Acylophorus*.

Key words. Acylophorina, Staphylininae, systematics, phylogeny, morphology, evolution, *Turgiditarsus eureka* sp.n., *T. vietnamensis* sp.n.

1. Introduction

The tribe Staphylinini is a monophyletic group of more than 5,500 predaceous rove beetle species (Brunke et al. 2016), which originated after the separation of Laurasia and Gondwana but no later than the Early Cretaceous (~137 Mya) (Brunke et al. 2017a). Despite containing some of the largest and most colorful taxa of the entire family, the systematics of Staphylinini has been heavily dependent on habitus until recently, derived mainly from the morphology of the pronotum (Brunke et al. 2016). Phylogenetic analyses of molecular and morphological data have shown that the evolution of a more cylindrical pronotum (classically subtribes Philonthina, Staphylinina, Xanthopygina, Anisolinina) from one that is shield-shaped (classically subtribe Quediina) has occurred multiple times, and frequently reversed to the plesiomorphic state (Solodovnikov 2006; Solodovnikov & Schomann 2009; Brunke et al. 2016; Chani-Posse et al. 2018). Examples of misplaced taxa include genera *Erichsonius* Fauvel, 1874 and *Stevensia* Cameron, 1932 which were, until recently, classified as members of Philonthina and Staphylinina, respectively. *Erichsonius* was recovered as a separate and morphologically isolated clade by Brunke et al. (2016), though supporting evidence was available as early as Smetana & Davies (2000), and therefore was given a separate, new subtribe. Although *Stevensia* (Fig. 1F) was not available to Brunke et al. (2016) for mo-

lecular data, it was found to possess all morphological characters of the newly resurrected Acylophorina and was transferred.

The usefulness of these new subtribe concepts in Staphylinini can be tested further by attempting to classify obscure taxa that were not explicitly considered or previously unavailable for study. One such taxon is the poorly known Oriental genus *Turgiditarsus* Schillhammer, 1997 which is, at present, known from 4 female specimens assigned to three species (Schillhammer 1996, 1997). The genus is remarkable for its exaggerated, boxing glove-like fifth protarsomere (Figs. 1A–E, 5D,E), unique among the beetles and with no known functional role. When the genus *Turgiditarsus* was described (originally under the preoccupied name *Tumiditarsus* Schillhammer, 1996), it was tentatively placed in the subtribe Anisolinina, based on the form of the pronotum and a superficial similarity to anisolinine genus *Pammegus* Fauvel, 1895 (Schillhammer 1996). The phylogenetic placement of this genus has not been revisited, likely due to its rarity and the absence of male specimens, which could provide character states that are phylogenetically informative within the new classification (Brunke et al. 2016; Chani-Posse et al. 2018).

Recent discovery and preliminary examination of a male specimen of *Turgiditarsus* revealed an absence of secondary structures on sternite VII, a weakly formed emargination of sternite VIII and a peculiar copulatory plate within the internal sac of the aedeagus, character states inconsistent with an assignment to Anisolinina (Chani-Posse et al. 2018). In order to phylogenetically place *Turgiditarsus*, we analyzed a matrix of both morphological and molecular data, broadly sampled across the lineages of Staphylinini. Although molecular data are still unavailable for many Staphylinini, including rarely collected *Turgiditarsus*, a total-evidence approach would allow these morphology-only taxa to be anchored within the recently resolved backbone topology of Staphylinini (Brunke et al. 2016; Chani-Posse et al. 2018).

2. Materials and methods

2.1. Abbreviations

Depositories. BMNH – The Natural History Museum, London, U.K. (M. Barclay, R. Booth); **CKB** – coll. Andreas Kleeberg, Berlin, Germany; **cSmet** – coll. Aleš Smetana, The National Museum of Nature and Science, Toshiba, Japan (S. Nomura); **CNC** – Canadian National Collection of Insects, Arachnids and Nematodes, Ottawa, Canada; **NHMB** – Naturhistorisches Museum, Basel, Switzerland (M. Borer, M. Geiser); **NHMW** – Naturhistorisches Museum, Wien, Austria; **USNM** – National Museum of Natural History, Smithsonian Institution, Washington D.C., U.S.A. (F. Shockley, D. Furth).

2.2. Microscopy and illustrations

Morphological specimens were examined using a Wild M5, Wild M10 and Nikon SMZ25 stereomicroscopes and were first relaxed in water before dissection of their terminal segments and genitalia. Genitalia were mounted on the same card as the specimen using fish glue. Line illustrations were made by hand using a camera lucida and a Leica DM 2500 microscope. Most illustrations were finished in Adobe Photoshop CS5 and Adobe Illustrator CC. Habitus photos and *Turgiditarsus* character photos were taken using a Nikon D4 in combination with a bellows and a reverse mounted Rodenstock Apo-Rodagon N 50/2.8 or a variety of Mitutoyo ELWD objectives and processed in Adobe Photoshop CS5. Other photos were taken using a motorized Nikon SMZ25 stereomicroscope and NIS Elements BR v4.5 for photomontage and photos were postprocessed in Adobe Photoshop CC. Tree diagrams were first formatted using FigTree v1.4.3 (http://tree.bio.ed.ac.uk/software/figtree/) and then finished in Adobe Illustrator CC. The distribution map was created using Google Earth. Measurements were taken using an ocular micrometer.

2.3. Phylogenetic analysis

2.3.1. Dataset

Forty-one taxa representing the major lineages of Staphylinini as recovered by Brunke et al. (2016) and Chani-Posse et al. (2018) were included in a total evidence matrix. *Arrowinus minutus* Solodovnikov & Newton, 2005 (tribe Arrowinini) was used as an outgroup taxon as in Chani-Posse et al. (2018). Molecular data from six gene fragments (nuclear protein encoding carbamoyl-phosphate synthetase, topoisomerase I, arginine kinase and wingless; mitochondrial protein encoding COI and nuclear ribosomal 28S) were used to create a concatenated alignment of 4556 bp. All molecular data was previously generated by either Brunke et al. (2016) or Chani-Posse et al. (2018) (see Table S1 for Genbank reference numbers) and we refer the reader to those publications for amplification, sequencing, and sequence editing and assembly protocols. Sequences were newly aligned in Geneious v10.2.3 using the MAFFT plugin v7.017, based on MAFFT (Katoh et al. 2002). 28S was aligned using the server version of Gblocks (Talavera & Castresana 2007) as in Chani-Posse et al. (2018). Individual gene alignments were concatenated with the 'concatenate' function of Geneious. Molecular data were unavailable for 5 taxa: *Turgiditarsus eureka* Schillhammer & Brunke, *Stevensia longipennis* Cameron, 1932 *Australotarsius grandis* Solodovnikov & Newton, 2009, *Acylophorus* (*Amacylophorus*) *pratensis* LeConte, 1863, and *Acylohsellus longiceps* (Cameron, 1918).

The morphological dataset was assembled in Mesquite v3.3 (Maddison & Maddison 2017) and consisted

Fig. 1. Habitus of: **A**: *Turgiditarsus vietnamensis* Schillhammer & Brunke, sp.n.; **B**: *T. ledangensis* Schillhammer; **C**: *T. kodadai* Schillhammer; **D**: *T. eureka* Schillhammer & Brunke, sp.n.; **E**: *T. chinensis* Schillhammer; **F**: *Stevensia longipennis* Cameron. — ***Scale bars***: 1 mm.

of 61 characters. Many characters were derived directly or with modification from previous matrices (Brunke & Solodovnikov 2013; Chani-Posse et al. 2018) but a significant portion were either novel in the taxonomic literature or described but never before used in a phylogenetic analysis (marked below with an *). The morphological characters used herein are a subset of a larger dataset in development by AJB.

2.3.2. Morphological characters

* indicates novel usage

1 Antennae, antennomere 1, anterior face*: (**0**) broadly glabrous; (**1**) densely setose with at most a narrow strip without setae. — Tomentose pubescence (far denser setation) considered as a different character state.

2 Antennae, antennomere 3, dense setation (**0**) absent; (**1**) present. — Tomentose pubescence (far denser setation) considered as a different character state.

3 Antennae, form: (**0**) non-geniculate between first and second segment; (**1**) geniculate between first and second segment.

4 Antennae, apical antennomere, broad microsetal sensory field (broad patch of pale, simple microsetae, longer than tomentose pubescence)*: (**0**) absent; (**1**) present and occurring on narrow face of segment, antennomere broadened to accommodate it (Fig. 2A,B). — Diverse other forms of sensory fields not considered homologous (setae arranged in a thin row in some *Quedius*, *Cyrtoquedius*, setae of different morphology (bead/scale-like or hooked apically in diverse Staphylinini Propria).

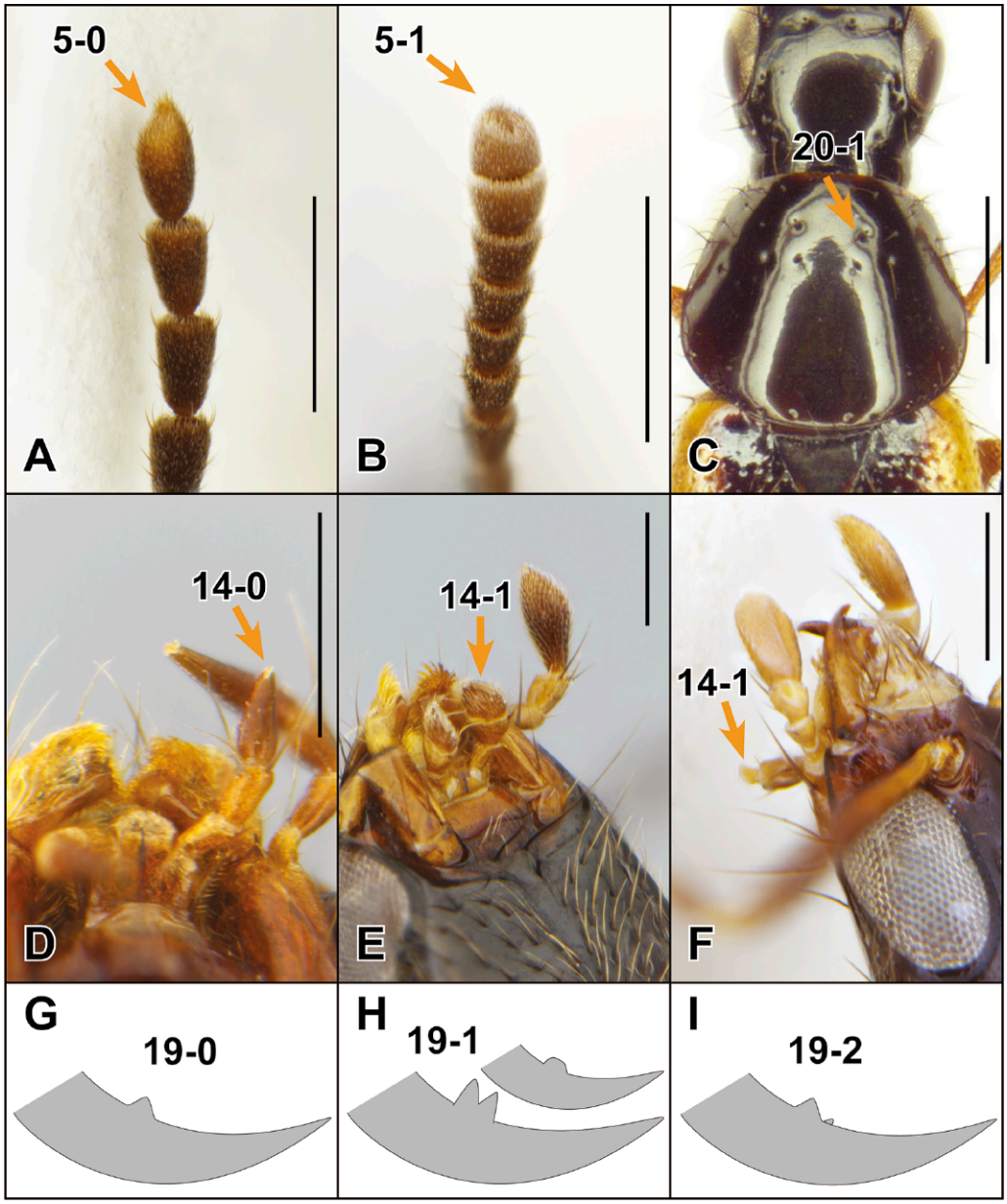

Fig. 2. Broad microsetose field of apical antennomere in: **A**: *Hemiquedius castoris* Brunke & Smetana (not expanded); **B**: *Acylophorus* sp., (expanded – partly sunken due to preservation). **C**: Second puncture of the dorsal row in *Quedius* (*Distichalius*) *bipictus* Smetana. Apical labial palpomere in: **D**: *Amacylophorus pratensis* (LeConte); **E**: *Acylophorus* sp.; **F**: *Acylohsellus longiceps* (Cameron). Right mandible, stylized character states of the basal teeth: **G**: single proximal tooth; **H**: bifid proximal tooth, sometimes fused into plate; **I**: proximal and distal tooth. — ***Numbers***: character-state combinations from the morphological matrix. — ***Scale bars***: A,B – 0.5 mm; C – 1 mm; D,E,F – 0.25 mm.

5 Antennae, apical antennomere, broad microsetal field, extension*: (**0**) occupying distinctly less than 40% of antennomere length, (Fig. 2A); (**1**) occupying 40% or more of antennomere length (Fig. 2B).

6 Antennal insertion, position: (**0**) away from level of anterior eye margin by > 2 × width of antennal socket; (**1**) away from level of anterior eye margin by 1.0–1.5 × width of antennal socket; (**2**) away from level of anterior eye margin by < 0.5 × width of antennal socket (touching or nearly touching eye margin; Fig. 2F).

7 Head, basal puncture (= vertical puncture of Smetana 1971)*: (**0**) absent; (**1**) present.

8 Parocular punctures (= oculomarginal punctures of Brunke & Solodovnikov 2014)*: (**0**) present; (**1**) absent.

9 Head and pronotum, microsculpture of transverse waves*: (**0**) absent; (**1**) present.

10 Head, ventral basal ridge, position (see Chani-Posse et al. 2018): (**0**) parallel with ventral part of post-occipital suture; (**1**) confluent with ventral part of post-occipital suture.

11 Head, postgenal ridge: (**0**) absent; (**1**) present.

12 Head, dorsal basal ridge: (**0**) absent; (**1**) present.

13 Head, labial palpi, dense brushes of setae on 2nd palpomere (see Brunke et al. 2016): (**0**) absent; (**1**) present.

14 Head, apical labial palpomere*: (**0**) not 'stub-like' in shape, either fusiform (Fig. 2D), aciculate or securiform (as in Fig. 1A,B); (**1**) with stub-like shape and truncate apex (Fig. 2E,F).
15 Head, gular sutures: (**0**) widely spaced and only weakly converging; (**1**) converging and narrowly spaced either at middle or further posteriorly.
16 Head, gula, distinct transverse basal impression (see Chani-Posse et al. 2018): (**0**) absent; (**1**) present.
17 Head, mandibles, shape (see Kypke et al. in press): (**0**) linear, lateral edge weakly curved; (**1**) curved, lateral edge strongly curved.
18 Head, mandibles, subapical tooth*: (**0**) present; (**1**) absent.
19 Head, right mandible, basal teeth*: (**0**) proximal tooth only, not bifid (Fig. 2G); (**1**) proximal tooth only, bifid often fused into a plate (Fig. 2H); (**2**) proximal tooth and distal tooth (Fig. 2I); (**3**) without teeth. — Several transitional states between a bifid proximal tooth and a broad flat extension occur in the genera *Anchocerus* and *Acylophorus*, they are therefore treated as the same state (2).
20 Prothorax, pronotum, second puncture of discal row (Fig. 2C)*: (**0**) absent; (**1**) present.
21 Prothorax, flexible postcoxal hypomeral extension or 'process': (**0**) absent; (**1**) present.
22 Prothorax, flexible postcoxal hypomeral extension or 'process', base*: (**0**) interrupted by inferior line; (**1**) not interrupted by inferior line.
23 Basisternum, pair of macrosetae: (**0**) absent; (**1**) present.
24 Basisternum, pair of macrosetae, distance from transverse ridge (see Chani-Posse et al. 2018): (**0**) distant, separated by a distance > 1 × puncture diameter; (**1**) approximate, separated by a distance < 1 × puncture diameter.
25 Prothorax, pronotum and prosternum (see Brunke et al. 2016): (**0**) pronotum not or only partially fused with prosternum in procoxal cavity; (**1**) pronotum completely fused with prosternum in procoxal cavity.
26 Prosternum, furcasternum, meshed microsculpture: (**0**) absent; (**1**) present.
27 Mesothorax, elytron, subbasal ridge, shape: (**0**) not forming a scutellar collar, extending to humerus; (**1**) not forming a scutellar collar, present as a short fragment only; (**2**) directed anteriad and forming 'scutellar collar'. — Situations where scutellar collar rudimentary but still visible and subbasal ridge extends to humerus, treated as state (2).
28 Mesothorax, mesoscutellum, posterior scutellar ridge: (**0**) absent; (**1**) present.
29 Mesothorax, mesoscutellum, vestiture*: (**0**) setose; (**1**) glabrous.
30 Mesothorax, elytron, row of humeral spines or spine-like setae: (**0**) absent; (**1**) present.
31 Mesoventrite, anterior half, isolated transverse ridge (see Chani-Posse et al. 2018): (**0**) absent; (**1**) present.
32 Mesothorax, epipleural row of setae in impressed punctures: (**0**) absent; (**1**) present.
33 Mesothorax, epipleural margin*: (**0**) uniform; (**1**) broadening anteriad.
34 Metatibia*: (**0**) spinose, at least 3 stout spines on outer face; (**1**) 0–2 thin spines on apical half of outer face.
35 Metacoxa, transverse carina: (**0**) absent; (**1**) present.
36 Protibia, spines on lateral face*: (**0**) present; (**1**) absent.
37 Profemur, lateroventral spines, apical row (see Chani-Posse et al. 2018): (**0**) present; (**1**) absent.
38 Protarsomeres, shape: (**0**) trapezoid, flattened; (**1**) cylindrical, not flattened.
39 Protarsi, claws, proportion: (**0**) no more than slightly larger than those of mid and hind legs; (**1**) at least twice as large than those of mid and hind legs.
40 Protarsomeres, ventral surface, tenent setae: (**0**) present, at least on basal segments; (**1**) absent.
41 Mesotarsomeres, number: (**0**) 5; (**1**) 4.
42 Mesotarsomeres: (**0**) trapezoid; (**1**) elongate, cylindrical and slightly flattened dorsally.
43 Metatarsomeres 2–5, surface of disc: (**0**) setose; (**1**) glabrous, except for marginal setae.
44 Empodial setae: (**0**) absent; (**1**) present.
45 Apical pretarsus, length of empodial setae relative to pretarsal claws: (**0**) about as long as on foreleg; (**1**) distinctly longer than on foreleg.
46 Hind wing, venation, veins CuA and MP4: (**0**) distinguishable as separate entities; (**1**) fused, not distinguishable.
47 Hind wing, venation, MP3: (**0**) present; (**1**) absent.
48 Metanotum, prototergal glands, cuticular manifestation, morphology: (**0**) shallow impression; (**1**) well-developed acetabulum.
49 Abdominal tergite III, posterior transverse basal carina: (**0**) present; (**1**) absent.
50 Abdominal tergite IV, impressed punctures at base and with glabrous area on most of disc*: (**0**) absent; (**1**) present.
51 Abdominal tergite IV, accessory basal lines: (**0**) absent; (**1**) present.
52 Abdominal sternite III, transverse carina, shape at middle*: (**0**) forming an obtuse angle, not produced posteriad; (**1**) forming an acute angle, sharply produced posteriad.
53 Abdominal sternite IV, transverse carina at middle: (**0**) straight, or rounded but not distinctly produced; (**1**) produced.
54 Male, abdominal sternite VIII, emargination: (**0**) present; (**1**) absent.
55 Male, basal mesotarsomere, brush of tenent setae (see Brunke & Solodovnikov 2013): (**0**) absent; (**1**) present.
56 Male: aedeagus, parameres, separation*: (**0**) separate, basal arms free; (**1**) fused, connected at least by the basal arms.
57 Male, aedeagus, paramere(s), sensory peg setae: (**0**) absent; (**1**) present.
58 Male, paramere*: (**0**) separated at the base from median lobe; (**1**) at least the base fused to median lobe.

59 Male, aedeagus, ventral, paired copulatory sclerite (see Brunke et al. 2016)*: (**0**) absent; (**1**) present.
60 Male, aedeagus, with well sclerotized, two-pronged copulatory piece (see Brunke et al. 2016)*: (**0**) absent; (**1**) present.
61 Male, aedeagus, external copulatory plate (Fig. 6)*: (**0**) absent; (**1**) present.

2.3.3. Bayesian phylogenetic analysis

The molecular portion of the matrix was initially partitioned by gene and codon position for protein-encoding genes. These candidate partitions were submitted to PartitionFinder v1.1.0 (Lanfear et al. 2012) to determine the optimal partitioning scheme and corresponding models of nucleotide evolution via the Bayesian Information Criterion. The settings were: all models, branch lengths unlinked, and search set to 'greedy'. Evolution in the single morphological partition was modeled using the Mkv model, with a gamma distribution. For the morphological partition, neither autapomorphic nor invariant characters were included in the dataset. The final matrix (4617 characters) combining molecular (4556 bp) and morphological data (61 characters) was analyzed by Bayesian inference in MrBayes v3.2.2 (Ronquist et al. 2012) running on the CIPRES Science Gateway v3.3 (phylo.org). Two runs of eight chains each were conducted over 30 million generations. Priors were mostly left at defaults except for modifications made by Brunke et al. (2016) and Chani-Posse et al. (2018). Initial over-mixing of the chains was remedied by changing the temperature paramere to default (temp=0.1) from 0.05, which usually improves convergence of total evidence datasets. Convergence was assessed using Tracer v1.6 (Rambaut et al. 2014) and by examining Potential Scale Reduction Factor (PSRF) and Average Standard Deviation of Split Frequency values (ASDSF) in the MrBayes output. Nodes with Bayesian posterior probability (PP) > 0.80 were considered well supported, nodes with PP = 0.70–0.80 were considered to be weakly supported, and nodes with PP < 0.70 were considered unsupported. Morphological character state transitions were optimized under parsimony on the fifty per cent majority rule consensus topology using the Trace over Trees function in Mesquite v3.3.

3. Results

3.1. Phylogenetic analysis

The partitioning scheme and corresponding models selected by PartitionFinder were: 1) 28S, and positions 1 and 2 of ArgK, CO1, CAD, TP and Wg – SYM+I+G; 2) position 3 of ArgK and Wg – GTR+I+G; 3) position 3 of CAD and TP – GTR+I+G; 4) position 3 of CO1 – HKY+G (identical to Brunke et al. 2016). After 30 million generations, the analysis clearly converged with ASDSF = 0.0044 and PSRF values = 1.003 (one parameter) or < 1.002 (all others). Overall, the recovered topology was well resolved with most nodes PP > 0.90 (Fig. 3). Within Staphylinini, South African *Afroquedius* Solodovnikov, 2006 was recovered as the sister group to the rest of the tribe with high support (PP=0.92), the southern hemisphere lineages Amblyopinina, Tanygnathinina, and Hyptiomina formed a well supported clade (PP=0.98) and Australian genus *Antimerus* Fauvel, 1878 formed the sister group to the Northern Hemisphere clade of Brunke et al. (2016) with moderately high support (PP=0.87). The Northern Hemisphere clade was recovered with maximal support (PP=1). Staphylinini Propria was maximally supported as monophyletic (PP=1) and all subtribes with more than one member included were maximally supported as monophyletic (PP=1). The topology within Staphylinini Propria was unresolved. A sister group relationship between Erichsoniina and Acylophorina was maximally supported (PP=1), and a sister group relationship between Indoquediina and the remaining taxa was moderately supported (PP=0.85). The sister group relationship between Erichsoniina and Acylophorina was also supported by a novel morphological character: antennomere inflated in narrow profile, bearing a broad field of pale, simple microsetae (4-1, see Methods).

Turgiditarsus was placed in Acylophorina with maximal support (PP=1) and possesses the morphological synapomorphies defining the subtribe (see clade 1 – Fig. 4, Results). *Turgiditarsus* is therefore transferred to Acylophorina. A sister group relationship between eastern North American *Hemiquedius* Casey, 1915 and southeast Palaearctic/Oriental *Turgiditarsus* was recovered with high support (PP=0.95). The sister group of Himalayan *Stevensia* within Acylophorina was unresolved. A sister group relationship between eastern North American *Anaquedius* Casey, 1915 and the remaining taxa was well supported by PP=0.91 (Fig. 3) and the loss of the emargination on male sternite VIII (clade 3 – Fig. 4). A sister group relationship between Australian genus *Australotarsius* and the remaining taxa (mostly Oriental) was well supported by PP=1 (Fig. 3) and by the setose scutellum, the loss of basisternal macrosetae and the loss of the external copulatory plate (clade 4 – Fig. 4). The *Acylophorus* lineage (see Taxonomy), was well supported by PP=1 (Fig. 3) and the presence of geniculate antennae and unequal pretarsal claws, and the fusion of CuA and MP4 wing veins (clade 5 – Fig. 4). The northeastern North American subgenus *Amacylophorus* Smetana, 1971 of *Acylophorus* Nordmann, 1837 (*Acylophorus pratensis*) was recovered outside of the genus *Acylophorus*, with high support (PP=1), as the sister group to the remaining *Acylophorus* lineage. This position was also supported by the fusiform apical labial palpomere, the unmodified protarsi bearing tenent setae, spinose metatibiae, the distal antennal insertions and the postcoxal process (clade 6 – Fig. 4). Therefore, we propose to raise the monobasic subgenus *Amacylophorus* to genus rank **stat.n.** (see 3.2.9.). *Anchocerus* Fauvel, 1905 was resolved as the sister group of a clade containing genera

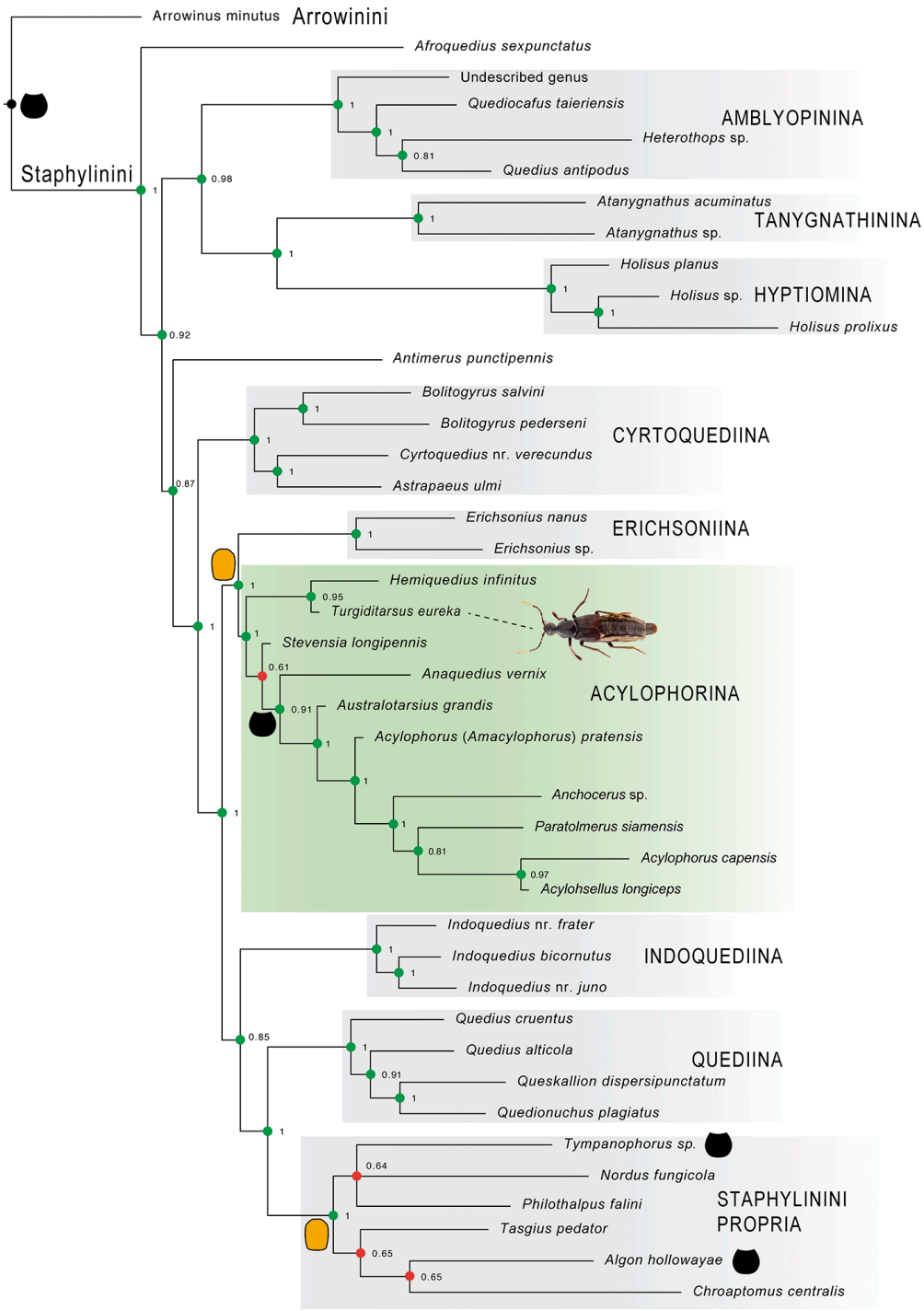

Fig. 3. 50%-majority-rule consensus tree from a partitioned, total evidence Bayesian phylogenetic analysis of six genes and morphology, with posterior probabilities to the right of the corresponding node. Multiple independent origins of pronotum shape indicated by icons. Nodes colored based on support from posterior probability (> 0.80 – green, 0.70–0.80 – yellow, < 0.70 – red).

Paratolmerus Cameron, 1932, *Acylohsellus* Smetana, 1995 and *Acylophorus* with moderate support (PP=0.81) (Fig. 3).

3.2. Subtribe Acylophorina Outerelo & Gamarra, 1985

Acylophorina Outerelo & Gamarra, 1985: 109 (only *Acylophorus*); Bouchard et al. 2011 (synonym of Quediina); Brunke et al. 2016 (re-validation of subtribe, redefinition, redescription, phylogeny); Chani-Posse et al. 2018 (as Acylophorina); Żyła & Solodovnikov 2017 (as Acylophorina).

Diagnosis. Members of this subtribe are recognized by the modified hind tarsus: tarsomeres elongate and simple (not bilobed), 2nd–5th slightly impressed dorsally, surface relatively glabrous, only a few macrosetae, each tarsomere with a dense, lateroapical row of spine-like setae, nearly all species with empodial setae of hind leg longer

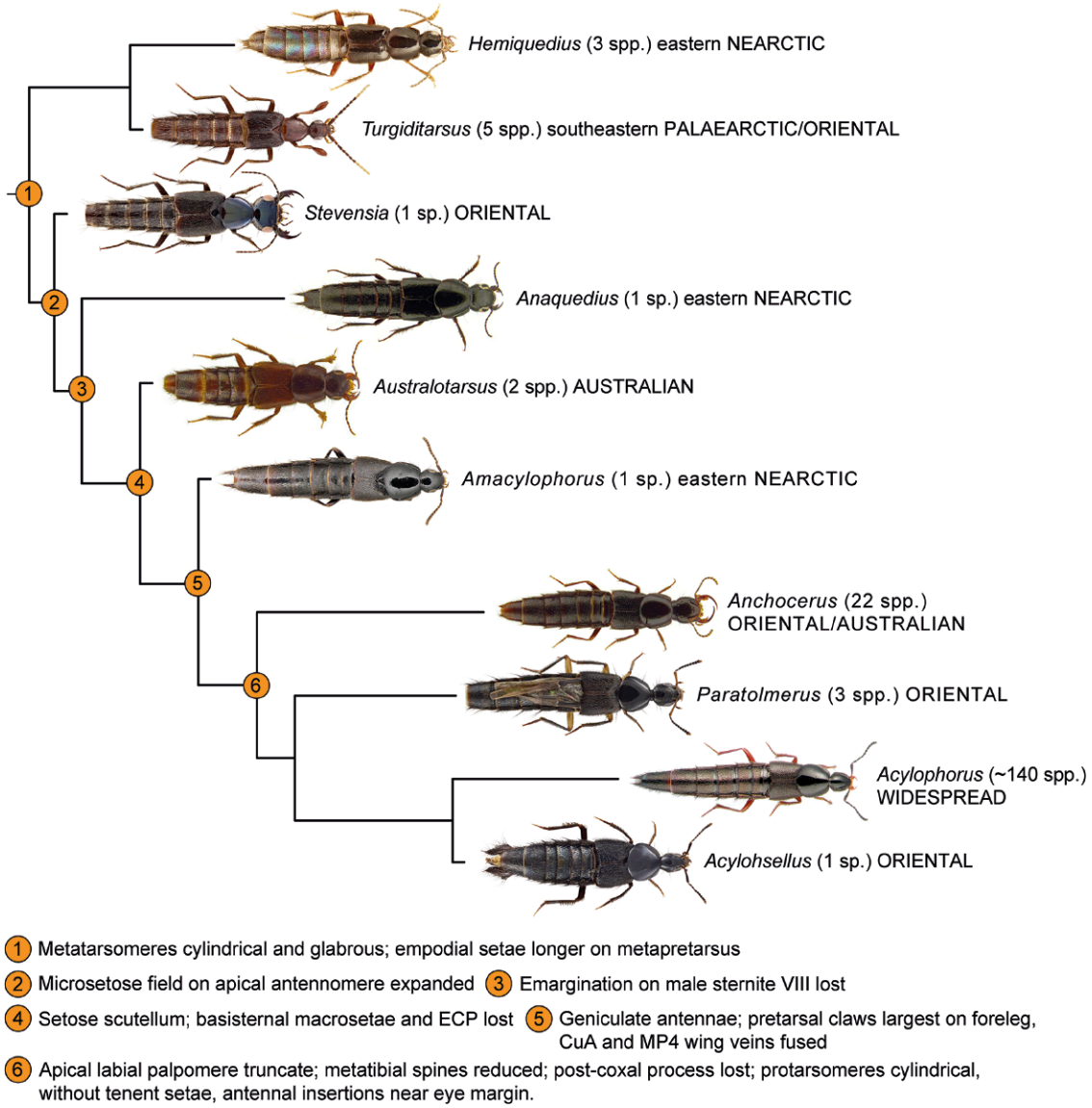

Fig. 4. Phylogeny and morphological evolution of the Acylophorina (Staphylinini) (topology from Fig. 3). Photo of *Acylophorus wagenschieberi* Kiesenwetter by K.V. Makarov. — ***Abbreviation***: ECP – external copulatory plate.

than that of foreleg (Brunke et al. 2016). Acylophorina are also distinctive for their apical antennomere, which is inflated in its narrowest profile (axis) to bear a broad field of pale, simple microsetae (Fig. 2A,B), a structure also found in their sister group, the Erichsoniina. A range of diverse, but different, structures (different field shape or structure of setae) were observed in various Staphylinini and warrant further study.

Genera included. *Acylohsellus* Smetana, *Acylophorus* Nordmann, *Amacylophorus* Smetana **stat.n.**, *Anaquedius* Casey, *Anchocerus* Fauvel, *Australotarsius* Solodovnikov & Newton, *Hemiquedius* Casey, *Paratolmerus* Cameron, *Stevensia* Cameron, and *Turgiditarsus* Schillhammer **new placement**.

The genera *Acylohsellus* (Smetana 1995a), *Anaquedius* (Smetana 1971), *Anchocerus* (Solodovnikov 2008), *Australotarsius* (Solodovnikov & Newton 2009) and *Hemiquedius* (Brunke et al. 2017b) are not redescribed herein and the reader is referred to the above-cited publications.

3.2.1. Key to genera of Acylophorina

1 Disc of elytra, at least medial half, glabrous between sparse rows of macrosetae; eastern North America … **2**

1' Disc of elytra uniformly setose; broadly distributed **3**

2 Protibia without spines; lateral parts of dorsal head with dense setae; sides of pronotum subparallel, only weakly converging anteriad (Fig. 4) .... ***Hemiquedius* Casey**

2' Protibia with several spines and apical spur; lateral parts of dorsal head without dense setae; sides of pronotum strongly converging anteriad (Fig. 4) .... ***Anaquedius* Casey**

3 Antennae geniculate **4**

3' Antennae not geniculate **8**

4 Apical labial palpomere fusiform and longer than previous palpomere (Fig. 2D); membranous post-coxal process present but small; protarsi with tenent

setae ventrally (at least on basal tarsomeres); antennal insertions far from anterior margin of eye, far more than 2 × the width of antennal socket; northeastern North America ..... ***Amacylophorus* Smetana**

4' Apical labial palpomere not fusiform, truncate apically and almost always shorter and narrower than previous palpomere (Fig. 2E,F); membranous postcoxal process absent; protarsi without tenent setae ventrally; antennal insertions near the level of anterior margin of eyes, no more than slightly farther than width of antennal socket; widespread **5**

5 With distinctive pair of punctures between the eyes, closer to each other than nearest eye; 1st antennomere with broadly glabrous anterior face (appearing dorsal if antennae reflexed); Oriental and Australasian Regions ..... ***Anchocerus* Fauvel**

5' With punctures between eyes near inner eye margin; 1st antennomere with, at most a narrow glabrous area; widespread **6**

6 Head evenly setose, except for center of disc; pronotal hypomeron at least partly visible in lateral view, especially near insertion of procoxa; disc of 4th metatarsomere with pair of long apical setae, usually exceeding last tarsomere, but at least 2/3 its length; Oriental Region ..... ***Paratolmerus* Cameron**

6' Head glabrous, with only macrosetae, temples usually densely, finely punctate; pronotal hypomeron not visible in lateral view; disc of 4th metatarsomere with only pair of very short apical setae **7**

7 Mandibles short, plate-like, apical portion reduced (Fig. 2F); males with dense patch of long setae on hind legs and specialized, velvety-patch on apical part of sternite VIII (see Smetana 1995a); apical labial palpomere always extremely reduced (Fig. 2F); Oriental Region, possibly east of Wallace's line .... ***Acylohsellus* Smetana**

7' Mandibles with long and thin apical portion of mandible, as typical for staphylinines; males without secondary sexual characters; apical labial palpomere of various widths; widespread .... ***Acylophorus* Gravenhorst**

8 Apical protarsomere greatly expanded and swollen (Fig. 5D,E); head < 0.5 × width of elytra (Fig. 1A–E); apical labial palpomere markedly expanded to apex; southeast Palaearctic, Oriental (non-Himalayan) .... ***Turgiditarsus* Schillhammer**

8' Apical protarsomere not swollen; head > 0.8 × width of elytra; apical labial palpomere fusiform; Oriental (Himalayan) and Australia **9**

9 Pronotum almost entirely glabrous, strongly shining; protarsi only weakly broadened (Fig. 1F); Himalayan region ..... ***Stevensia* Cameron**

9' Pronotum evenly setose; protarsi markedly broadened (Fig. 4); Australia (including Tasmania) .... ***Australotarsius* Solodovnikov & Newton**

3.2.2. *Turgiditarsus* Schillhammer, 1997
(Figs. 1A–E, 5A–E, 6A–D, 7 (map))

Turgiditarsus Schillhammer, 1997: 109, replacement name for preoccupied *Tumiditarsus* Schillhammer, 1996
Tumiditarsus Schillhammer, 1996: 63 (as Staphylinini: Anisolinina)

Type species. *Turgiditarsus ledangensis* Schillhammer.
Diagnosis. *Turgiditarsus* can be easily identified by the expanded apical protarsomere, unique within Staphylininae.
Redescription. We here supplement or partly repeat the original description in Schillhammer (1996) with respect to some phylogenetically relevant morphological character states: dorsal forebody without microsculpture; antennomeres 1–3 with dense setation; antennae non-geniculate; apical antennomere not shorter than penultimate, inflated in narrow profile; microsetose field of apical antennomere present but not expanded to 40% or more of segment; antennal insertion far from anterior margin of eye; dorsal basal ridge absent; mandibles with proximal tooth formed as a plate; prosternum with pair of basisternal macrosetae; postcoxal process present and delimited at base by inferior marginal line; scutellum glabrous or punctate; wing with veins CuA and MP4 distinguishable as separate entities; protibia with apical spurs but without spurs on lateral face; empodial setae distinctly longer on mid and hind leg than foreleg; protarsal claws not enlarged or proportionally larger than on other legs; protarsomeres I–IV trapezoid and flattened, with tenent setae; metatibia with stout spines on lateral face; metacoxae without transverse carina; metatarsomeres elongate, cylindrical and slightly flattened dorsally, II–V glabrous on disc; abdominal sternite III with transverse carina sharply produced and forming an acute angle; male sternite VIII with shallow emargination; male aedeagus with external copulatory plate.
Distribution. The genus is thus far known from lowland subtropical and tropical forests, ranging from Chongquing to Zhejiang, China, south to Vietnam, peninsular Malaysia and Borneo (Fig. 7).
Comments. The discovery of the first male *Turgiditarsus* demonstrates that the strongly enlarged and modified protarsus is not sexually dimorphic and is unlikely to function in pre-mating behavior or copulation. The protarsus may be modified for a specialized mode of prey capture, targeting prey with either a rapid escape response or a difficult to grip body. The groove on the underside of the protarsus suggests that some sort of secretion may be involved but no histological investigations have been attempted.

3.2.3. Key to species of *Turgiditarsus*

1 Scutellum impunctate **2**

1' Scutellum punctate **3**

2 Body black (Fig. 1A); Vietnam .... ***T. vietnamensis* Schillhammer & Brunke, sp.n.**

2' Body reddish brown (Fig. 1B); peninsular Malaysia ..... ***T. ledangensis* Schillhammer**

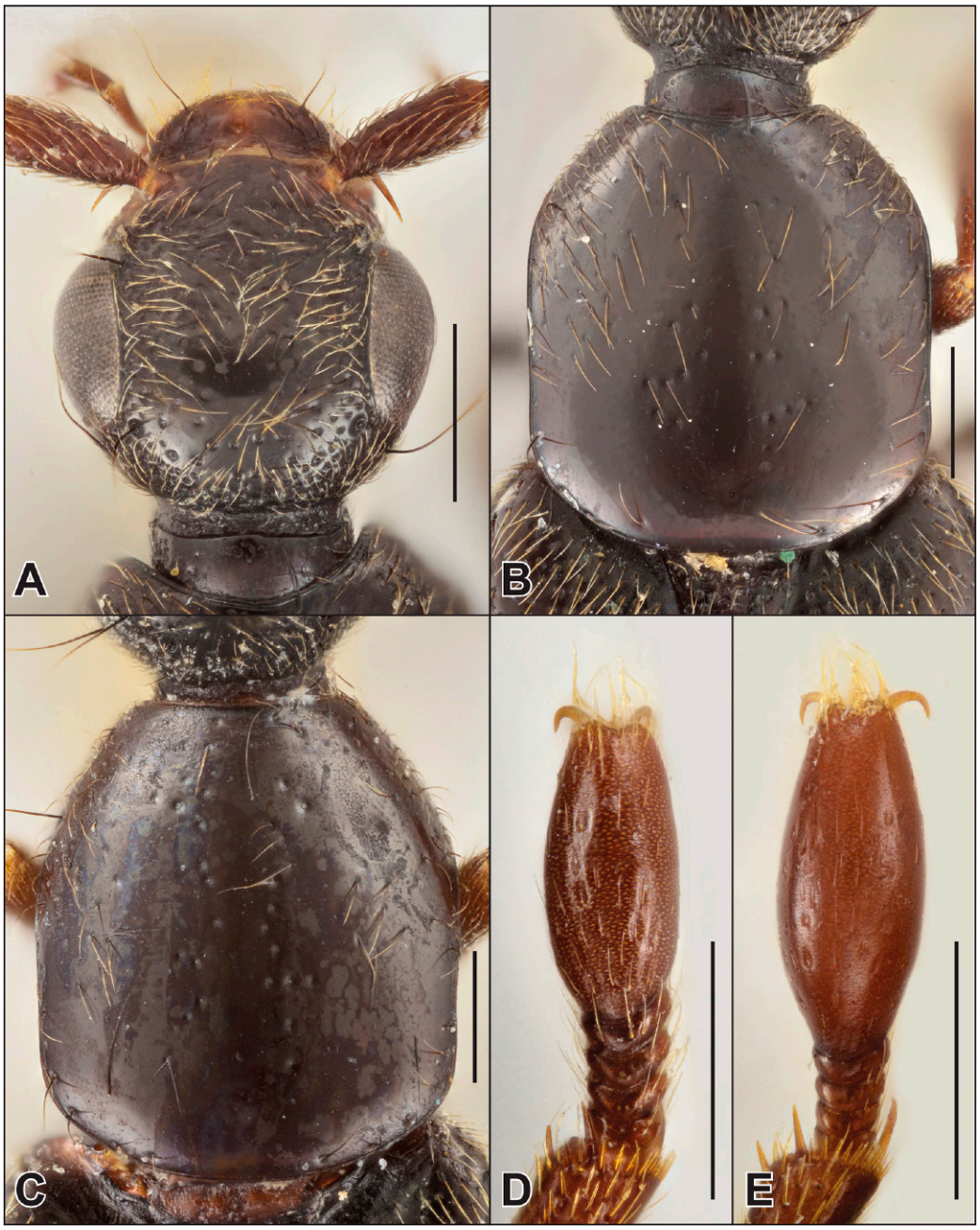

Fig. 5. Dorsal views of head (**A**), pronotum (**B**,**C**) and foretarsus (**D**,**E**) of *Turgiditarsus* Schillhammer: *T. eureka* Schillhammer & Brunke (**A**,**B**,**D**) and *T. chinensis* Schillhammer & Brunke (**C**,**E**). — ***Scale bars***: 0.5 mm.

3 Pronotum densely, uniformly and strongly punctate; body (including legs) black, three distal antennomeres whitish (Fig. 1C); Borneo ..... ***T. kodadai* Schillhammer**

3' Pronotum with two irregular rows of few punctures, majority of pronotal disc impunctate; abdominal segments partly and legs reddish brown, four distal antennomeres whitish; China **4**

4 Pronotum wider, 1.06 × as long as wide (Figs. 1D, 5B); Chongqing Province, China ..... ***T. eureka* Schillhammer & Brunke, sp.n.**

4' Pronotum narrower, 1.14 × as long as wide (Figs. 1E, 5C); Zhejiang Province, China ..... ***T. chinensis* Schillhammer**

3.2.4. *Turgiditarsus eureka* Schillhammer & Brunke, sp.n.

(Figs. 1D, 5A,B,D, 6A–C, 7 (map))

Material examined. ***Type material***: Holotype ♂, 'Ta-ning-ho | Sze-chuan E.B. | May-June, 1904', '6512', '? genus sp.', 'HOLOTYPE | *Turgiditarsus* | *eureka* sp.n. | des. Schillhammer | & Brunke 2017' (USNM).

Diagnosis. Externally, the species is almost identical with *T. chinensis* Schillhammer, 1996 but differs by the broader pronotum (1.14 × as long as wide in *T. chinensis*, see Fig. 5), and by the different shape of tarsomere 5 (Fig. 5D for *T. eureka*, Fig. 5E for *T. chinensis*).

Description. 9.5 mm long (4.7 mm, abdomen excluded). Head, pronotum and elytra black, lateral and posterior margins and hypomera of pronotum, posterior margin and epipleural part of elytra obscurely reddish brown; abdomen dark brown to blackish (pigmentation may have faded due to age of specimen), posterior margins of segments III–V broad obscurely reddish, posterior halves of segments VI–VIII obscurely reddish; labrum dark reddish brown but distinctly paler medially; mandibles and palpi pale reddish brown; first antennomere dark reddish brown, antennomere 2 black, narrowly reddish distally and with reddish constricted portion at base, antennomeres 3–7 black, antennomeres 8–11 creamy white; legs with femora black with indistinct dark reddish patch distally, tibiae reddish, medial faces of meso- and metatibiae infuscate, tarsi reddish.

Head suborbicular, 1.05 × as wide as long, moderately strongly, densely punctate, except vertex where punctuation is sparse but coarse; eyes 2.4 × as long as tempora; pronotum subparallel-sided, 1.06 × as long as wide, sides indistinctly concave, surface flat, antero-lateral portion strongly deflexed, along midline with two rows of irregularly arranged fine punctures, a moderately dense group of punctures sublaterally, densely punctate at anterior angles, posterior fifth impunctate; both head and pronotum without microsculpture, but surface of pronotum with microscopic stitches.

Elytra much broader and along sides much longer than pronotum, densely punctate, punctures separated by about a puncture diameter; scutellum moderately densely punctate, punctures smaller than those on elytra.

Abdominal tergites densely punctate, density decreasing toward apex of abdomen, punctural grooves drop-shaped on basal tergites, gradually becoming narrower and longer distad, tergite III with distinct transverse depression at base.

Aedeagus (Fig. 6A–C) with median lobe rather short and stubby, in lateral view with narrow and well separated apex; paramere (Fig. 6C) deeply bilobed, lobes broad, well separated, each lobe with numerous, tightly packed peg setae in distal half.

Distribution. The species is at present known only from the type locality in northeastern Chongqing, China (Fig. 7). ***Note on the type locality***: Taning Ho is a river in northeastern Chongqing province of China, flowing into the Yang Tse River at the City of Wushan. The locality is situated roughly 1000 km west of the type locality of *T. chinensis*.

Derivatio nominis. The specific epithet describes the authors' first reaction at beholding the first male specimen of this genus, eventually enabling them to solve the puzzle of its systematic position. It is the transcription of a Greek exclamation, thus indeclinable.

3.2.5. *Turgiditarsus vietnamensis* Schillhammer & Brunke, sp.n.

(Figs. 1A, 6D, 7(map))

Material examined. ***Type material***: Holotype ♀, 'VIETNAM-N, Quang Binh prov. | 1km N of Cha Lo, 400 m | Vietnam-Laos border area | 17°41′22″N 105°45′45″E | L. Dembický leg., 11.–24. iv.2010', 'HOLOTYPE | *Turgiditarsus* | *vietnamensis* sp.n. | des. Schillhammer | & Brunke 2017' (NHMB).

Diagnosis. *Turgiditarsus vietnamensis* differs from the only other known species with an impunctate scutellum, *T. ledangensis*, in the larger body size, dark coloration, the slightly broader scutellum and the styli of tergite IX with convex outline (more or less conical in *T. ledangensis*).

Description. 11.5 mm long (5.1 mm, abdomen excluded). Head, pronotum, elytra and abdomen black, segment VIII of abdomen dark reddish brown; labrum reddish brown but with two large patches on either side of middle darker; mandibles and palpi pale reddish brown; antennae with antennomeres 1–7 black, antennomere 8 dark brown, narrowly whitish distally, antennomeres 9–11 creamy white; legs black, protibiae and all tarsi dark reddish to reddish brown.

Head suborbicular, 1.1 × as wide as long, rather coarsely and densely punctate, except vertex which is impunctate; eyes 1.7 × as long as tempora; pronotum 1.18 × as long as wide, widest slightly in front of midlength, slightly narrowed toward base in almost straight line, surface weakly convex, antero-lateral portion strongly deflexed, along midline with two rows of irregularly arranged punctures, right row with two, left row with four punctures, with a larger lateral seta at about midlength similar in size to large anterior lateral seta, rather densely punctate in anterior fourth behind anterior angles; both head and pronotum without microsculpture, but surface of pronotum with microscopic stitches.

Elytra much broader and along sides much longer than pronotum, densely punctate, punctures separated by about a puncture diameter; scutellum impunctate.

Abdominal tergites variably densely punctate, densely on tergite III, less densely on subsequent tergites, generally punctures at base of tergites denser but very fine, remaining punctural grooves drop-shaped on basal tergites, gradually becoming narrower and longer distad, tergite III with indistinct transverse depression at base. Female tergite × (Fig. 6D) with apex truncate and medially produced, apical margin with a dense row of rather long setae; disc with indistinctly delimited patch of dark brown pigmentation.

Distribution. The species is at present known only from the type locality in southern North Vietnam (Fig. 7).

Derivatio nominis. The species is named after the country of its origin.

3.2.6. *Stevensia* Cameron, 1932

(Fig. 1F)

Stevensia Cameron, 1932: 162 (as Philonthina); Herman 2001 (as Quediina); Schillhammer 2004 (as Staphylinina); Schillhammer 2011 (as Staphylinina); Schülke & Smetana 2015 (as Quediina); Brunke et al. 2016 (as Acylophorina).

Type species. *Stevensia longipennis* Cameron.

Diagnosis. Easily recognized within the subtribe by a combination of: evenly setose elytra; non-geniculate

antennae; nearly glabrous pronotum and head, which is broader than the pronotum.

Redescription. We here focus on phylogenetically relevant characters, for additional details see species redescription below. Antennae non-geniculate; apical antennomere shorter than penultimate; postcoxal process present and delimited at base by inferior marginal line; basisternal setae present; scutellum glabrous; foretibia with apical spurs and lateral spines; protarsi flattened, bilobed and with tenent setae; protarsal claws not enlarged or proportionally larger than on other tarsi; CuA and MP4 wing veins separate; abdominal sternite III with basal transverse carina sharply produced at middle; male sternite VIII with weak emargination; male aedeagus with external copulatory plate.

Distribution. The genus appears to be confined to the Himalayan subregion of the Oriental region.

3.2.7. *Stevensia longipennis* Cameron, 1932
(Figs. 1F, 6E–G, 7 (map))

Stevensia longipennis Cameron, 1932: 162 (India: Sikkim); SCHILLHAMMER 2004 (Nepal); SCHILLHAMMER 2011 (Bhutan, India: West Bengal).

Material examined. ***Type material***: 8 syntypes (2 ♂, 6 ♀), 'Sikkim | Gopaldhara, Rungbong Vall. | H. Stevens', 'H. Stevens | Brit. Mus., 1922…307' (BMNH). — ***Other material***: NEPAL: Kathmandu V., Burhanilkanth, 1440–1650 m, 16,VI.1983, M. Brancucci (1 ♂, NHMB); E-Nepal, env. Shivalaya, bank of Kimti Khola, 2.5.1993, leg. A. Kleeberg, (1 ♂, CKB). BHUTAN: Wangdi Phodrang Prov., 44 km SSE Whangdi Phodrang, Nyara Chhu, ca 550 m, 27°10′22″N 90°3′48″E, 25.XI.2005, leg. M. Jäch (22) (2 ♀, NMW). INDIA: NE India, Arunachal Pradesh, 8 km S Jamira – SESSA vicinity, 27°07′–09′N 92°34′E, 350 m, L. Dembický leg., 26.V.–4.VI.2005, BMNH 2006-48 (1 specimen, BMNH).

Redescription. Habitus: Fig. 1F. 11.0–13.1 mm long (6.5–7.0 mm, abdomen excluded). Black, distal one or two maxillary palpomeres, mandibles partly, labrum, posterior margin of elytra and tergite VIII obscurely reddish brown, margins of labrum yellowish brown. Head with dark steel blue sheen, pronotum with dark greenish sheen.

Head transverse, 1.55–1.65 × (males) or 1.30–1.40 × (females) as wide as long, eyes large, weakly prominent, about 1.5–1.8 × as long as regularly convex tempora. Along ventral margin of eyes with sharp ridge extending to about half eye width at posterior margin of eyes; medial margin of eyes with hardly discernible line indicated by exceedingly fine stitches. Dorsal surface glossy, with pair of flat but conspicuous depressions between eyes. Tempora with dense, short, silvery pubescence. Anterior margin of clypeus broadly, shallowly emarginate. Labrum short, broad, lobes apparently fused but with medial notch and a clearly visible median separation line; transparent marginal portion very narrow medially, becoming broader laterally; mandibles long and slender, medial margin of left mandible with three teeth, that of right mandible with one bicuspid tooth. Maxillary and labial palpi moderately long, slender, second labial palpomere with one medial seta and a bunch of four setae clustered at distal margin. Antennae long, slender, all segments much longer than broad, six outer antennomeres slightly cone-shaped.

Pronotum about as long as wide, in most specimens inconspicuously wider than long, widest slightly in front of midlength, distinctly narrowed in almost straight line toward obtuse but well demarcated hind angles. Surface glossy, but with a pair of admedian punctures at anterior third. Marginal punctures fine, sparse, bearing very fine but long setae. Head and pronotum without any traces of microsculpture but with sparse, microscopically fine stitches.

Elytra very long, much longer than pronotum, subparallel-sided. Punctation strong, dense, punctures separated by about a puncture diameter, bearing rather short and stout yellowish setae. With two long lateral macrosetae slightly posteriad of shoulder. Humeral angle with short carina bearing a small cluster of short and stout black setae. Scutellum impunctate and without microsculpture.

Abdominal tergites with only one basal line. Tergite III densely punctate and pubescent, punctation becoming less dense posteriorly, tergites IV–VI with anterior third densely punctate and pubescent, posterior two thirds much less densely punctate, becoming almost impunctate toward apical tergites; tergite VII with anterior fourth densely punctate and pubescent, posterior third slightly less densely punctate, area in between sparingly punctate, medially narrowly impunctate; pubescence short and uniform on tergite III, becoming increasingly longer on each subsequent tergite, tergite VII with two semi-erect tufts of long setae on each side of impunctate median area. Tergite VIII with anterior third densely punctate and with rather short pubescence, posterior two thirds less densely punctate but with pubescence becoming longer posteriad. Sternites with very dense and long lateral pubescence, with long setae in postero-lateral angles.

Male sternite VIII with very shallow and rather narrow asetose medio-apical emargination and short semimembranous portion; disc with two pairs of very long macrosetae.

Aedeagus (Fig. 6E,F) slender, cylindrical; paramere (Fig. 6E,G) almost as broad as median lobe, subparallel-sided, medio-apically shortly and narrowly split, with a narrow fissure near base, with numerous peg setae arranged in two rough clusters near apex, with four pairs of apical setae. Internal sac with bell-shaped and everted external copulatory plate (Fig. 6E,F).

Distribution. The species has been recorded from northeastern India (West Bengal, Arunachal Pradesh), eastern Nepal, and Bhutan (Fig. 7). Available data suggests that it occurs in mountain valleys of the Himalayas, at least sometimes near running water (riverbank). Note on type locality: The type locality is actually located in Darjeeling, West Bengal.

Comments. The specimens from Bhutan and Arunachal Pradesh have notably shorter tempora (1.5 × as long as eyes versus 1.7–1.8 ×) than those from Darjeeling. However, it is not possible to judge whether this is a consistent difference without additional material.

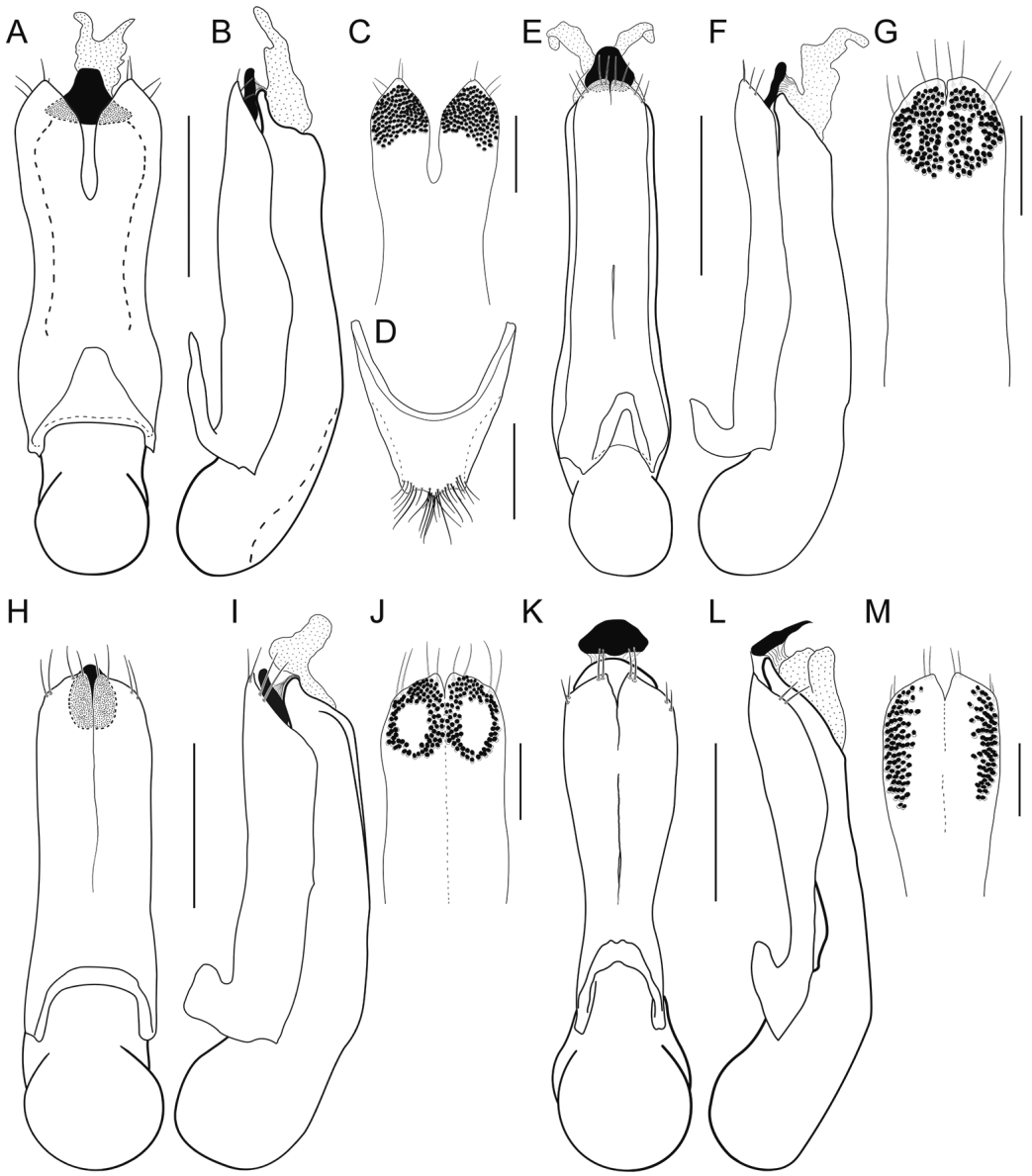

Fig. 6. Aedeagi of Acylophorina with an external copulatory plate (solid black) and female tergite X. Aedeagus in ventral (**A**,**E**,**H**,**K**) and lateral (**B**,**F**,**I**,**L**) view, and paramere (**C**,**G**,**J**,**M**) of: *Turgiditarsus eureka* Schillhammer & Brunke (**A**–**C**); *Stevensia longipennis* Cameron (**E**–**G**); *Anaquedius vernix* (LeConte) (**H**–**J**); *Hemiquedius castoris* Brunke & Smetana (**K**–**M**). Female tergite X (**D**) of *Turgiditarsus vietnamensis* Schillhammer & Brunke. — ***Scale bars***: aedeagi – 0.5 mm; parameres and female tergite X – 0.25 mm.

3.2.8. The *Acylophorus* lineage
(Fig. 4 – clade 5)

The genera *Acylophorus*, *Anchocerus*, *Paratolmerus* and *Acylohsellus* formed a well-supported monophyletic clade in the analysis and share protarsal claws larger than those of other legs, fused CuA and MP4 wing veins and characteristic geniculate antennae (Fig. 4). This clade is defined here as the *Acylophorus* lineage and encompasses all '*Acylophorus*-like' taxa in Acylophorina. This is the most speciose lineage in the subtribe, with *Anchocerus* including 22 species and *Acylophorus* **sensu n.** including about 140 described species (Fig. 4). *Amacylophorus* **stat.n.**, previously a subgenus of *Acylophorus*, is here raised to genus rank based on the results of our analysis and is included in this group.

Genera included. *Acylohsellus* Smetana, *Acylophorus* Nordmann, *Amacylophorus* Smetana **stat.n.**, *Anchocerus* Fauvel and *Paratolmerus* Cameron.

3.2.9. *Amacylophorus* Smetana, 1971 stat.n.
(Figs. 2D, 4)

Amacylophorus Smetana, 1971: 247 (subgenus of *Acylophorus*); Smetana 1981 (Ontario, Canada, habitat); Webster et al. 2012 (New Brunswick, Canada, habitat).

Type species. *Amacylophorus pratensis* (LeConte).
Diagnosis. *Amacylophorus* can be recognized by a combination of: geniculate antennae; antennal insertions distant from anterior eye margin; and the fusiform apical labial palpomere.

Redescription. Antennae geniculate; first antennomere with only sparse setae; apical antennomere inflated in narrow profile, reduced in size, with broad microsetose field occupying more than 40% of segment; antennal insertion distant from anterior eye margin; apical labial palpomere fusiform, longer than previous segment; mandible with basal tooth bifid; postcoxal process small but present, not interrupted by interior marginal line; basisternum without pair of macrosetae; scutellum setose; metatibia with 4 stout spines on outer face; protibia with lateral spines; protarsomeres not cylindrical, with tenent setae ventrally on basal 4 (male) or 2 (female) segments, with pretarsal claws distinctly larger than those of other legs; metatarsomeres elongate, cylindrical and slightly flattened dorsally, segments II–V glabrous dorsally, with empodial setae distinctly longer than those of foreleg; wing veins CuA and MP4 fused; abdominal sternite III with transverse basal line sharply projected at middle; apex of male sternite VIII without emargination; males without external copulatory plate in internal sac of the aedeagus.

Distribution. Northeastern North America: Newfoundland and New Brunswick west to Minnesota, east to New England (Massachusetts, New Hampshire) (Smetana 1971; Smetana 1981; Webster et al. 2012). The local distribution of its only species, *Amacylophorus pratensis*, may be very patchy as it appears to prefer cold and wet microhabitats in fens (neutral/alkaline, nutrient-poor), forested swamps (Webster et al. 2012) and other wetlands, especially with relict boreal plant assemblages in the southern part of its range. Its distribution matches the classic 'postglacial fringe' distribution of glacial relict Pselaphinae in North America that are neither true boreal nor widespread deciduous forest faunal elements (Reichle 1996).

Comments. Several morphological features of *Amacylophorus* (Fig. 4), now known to be inconsistent with the remaining genera in the *Acylophorus* lineage, were already mentioned by Smetana (1971) as notable (broad tarsi with tenent setae, long apical labial palpomere, antennal insertions distant from level of anterior eye margin) and used as justification for erecting a new subgenus. The results from the phylogenetic analysis indicate that these differences support a position as sister to the other genera of the *Acylophorus* lineage. Additional features inconsistent with *Acylophorus* itself include a relatively short first antennomere with only sparse setae and a broad paramere, with peg setae arranged in whirled patterns (similar to *Anaquedius* or *Stevensia*, see Fig. 6).

3.2.10. *Paratolmerus* Cameron, 1932
(Fig. 4)

Paratolmerus Cameron, 1932: 169; Smetana 1988 (redescription, key, *Acylophorus*-lineage); Rougemont 1991 (species from Thailand); Brunke et al. 2016 (phylogeny, member of Acylophorina); Smetana 2018 (species from Hainan, China).

Type species. *Paratolmerus pilosiventris* Cameron, 1932.

Diagnosis. *Paratolmerus* can be distinguished from other genera of the *Acylophorus* lineage by a combination of: hypomeron of pronotum with small to large extension at level of procoxal insertion, partly visible in lateral view; head evenly punctate except for glabrous center; and pair of long setae on the 4th metatarsomere, 2/3 the length of the last segment (*P. siamensis* Rougemont) or longer than this segment (other species).

Redescription. The genus was redescribed in detail by Smetana (1988) but we here supplement this account: dorsal head nearly entirely covered with setose punctures; antennae geniculate; first antennomere densely setose; third antennomere densely setose; apical antennomere inflated in narrow profile, shortened and bearing broad microsetose field occupying more than 40% of its length; antennal insertion close to eye margin, separated by about one antennal socket width or slightly more; apical labial palpomere reduced to short and thin stub, truncate at apex; proximal tooth of right mandible bifid; membranous postcoxal process absent, with non-homologous, small to large and triangular, sclerotized extension at level of forecoxa, visible in lateral view; basisternum without pair of macrosetae; scutellum setose; protibia with spines on lateral face; metatibia entirely lacking spines; protarsomeres cylindrical and without tenent setae ventrally, with pretarsal claws larger than those of mid and hind legs; metatarsomeres elongate, cylindrical and slightly flattened dorsally, segments II–V glabrous dorsally, with empodial setae distinctly longer than those of foreleg; fourth metatarsomere with long (2/3 the length of last segment in *siamensis*) or extremely long (longer than last segment, other species) pair of setae; wing veins CuA and MP4 fused; abdominal sternite III with transverse basal line sharply projected at middle; apex of male sternite VIII without emargination; males without external copulatory plate in internal sac of the aedeagus.

Distribution. Known from the Himalayas (type species), mainland southeast Asia (*P. siamensis*, Rougemont 1991) and from Hainan, China (*P. primigenius* Smetana, Smetana 2018). Species have been collected from wet litter in small tropical forest streams (Smetana 1988; Rougemont 1991; Smetana 2018).

Comments. The type species of the genus, *P. pilosiventris* Cameron, 1932, is notably different in appearance from the other two known species of the genus: southeast Asian *P. siamensis* and southern Chinese *P. primigenius* (Smetana 2018). The forebody is even more convex, the mandibles are much larger, the visible hypomeral extension is greatly enlarged to form a process similar but not homologous to that of paederines, and the head is very densely punctate. Nevertheless, all three species share the distinctively outflexed hypomeron, the punctate head and pair of long setae on tarsomere 4. The relationship of *Paratolmerus* to *Acylophorus* was outside of the scope of the present analysis, and it is possible that the former is derived from within the latter. The presence of a pair of long tarsal setae in Himalayan *Acylophorus siyo* Smetana, 1988, an otherwise typical member of the genus,

supports this. The triangular extension of the hypomeron in *P. pilosiventris* is not considered to be homologous with the postcoxal process found in many Staphylinini as it is entirely opaque and located in line with the coxal articulation (i.e., not 'postcoxal'). Smetana (1988) stated that the empodial setae were quite short in *P. pilosiventris* but a re-examination of this specimen has shown the empodial setae to be broken on all but one tarsus, where they are of typical length for the subtribe (longer than those of the protarsus). Several *Acylophorus* species with a setose head (African *A. kambuiensis* Bordoni, 1994 and *A. lualabaensis* Levasseur, 1968; Asian *A. puncticeps* Fauvel, 1895 and *A. hayashii* Smetana, 1995) were unavailable for examination and may prove to be *Paratolmerus*.

3.2.11. *Anchocerus* Fauvel, 1905
(Fig. 4)

Anchocerus Fauvel, 1905: 141; Smetana 1988 (redescription); Solodovnikov 2008 (review and redescription); Hu et al. 2012 (new species, updated key to Chinese species); Brunke et al. 2016 (phylogeny, member of Acylophorina); Janak 2017 (new species, novel morphological variation).

Type species. *Anchocerus birmanus* Fauvel, 1905.
Diagnosis. *Anchocerus* can be distinguished by others of the *Acylophorus* lineage by a combination of the weakly constricted neck and a pair of punctures between the eyes that are closer to each other than to the inner eye margin.
Morphological variation. Recent taxonomic work on *Anchocerus* (Janak 2017) and the examination of additional specimens has revealed that most characters listed by Solodovnikov (2008) to define *Anchocerus* either need modification or are no longer entirely diagnostic. The weakly constricted neck also occurs in some New World species of *Acylophorus* (e.g., those related to *Ac. caseyi* Leng, 1920) and *Amacylophorus pratensis*. The length of the first antennomere is too variable to be reliably diagnostic of the genus as some *Anchocerus* in Janak (2017) have this segment much longer than the following 2–3 segments. In all *Anchocerus* studied, the anterior face of the first antennomere is broadly glabrous, though the rest of the segment may bear many small setae. The typical left (usually both) mandible of *Anchocerus* bears a plate-like 'tooth' but *An. differens* Janak, 2017 has only a minute sharp tooth and *An. rougemonti* Janak, 2017 has a sharp, acute plate, appearing intermediate between the typical rounded plate and the bifid tooth of other genera (Janak 2017). The empodial setae of the hind leg are longer than the pretarsal claws in several *Anchocerus* species of different sizes, overlapping with the variation present in *Acylophorus.* The pair of approximate punctures between the eyes occurs in all *Anchocerus* known to us and is unique within the *Acylophorus* lineage. The dense setation of antennomere 3, a character state found throughout Acylophorina and Erichsoniina, is variable within the genus and many species have only a few macrosetae.
Distribution. *Anchocerus* species are known from the Oriental region south to New Guinea and north-eastern Australia.

3.2.12. *Acylophorus* Fauvel, 1905 sensu n.
(Figs. 2B,E, 4)

Acylophorus Nordmann, 1837: 127; Bierig 1938 (Neotropical fauna, subgenera); Smetana 1971 (North American fauna, subgenera); Smetana 1988 (Himalayan fauna); Smetana 1995b (Taiwanese fauna); Lott 2010 (Afrotropical fauna).

Type species. *Acylophorus glaberrimus* Herbst, 1784.
Diagnosis. *Acylophorus* is distinguished from other genera in the *Acylophorus* lineage by a combination of: apical labial palpomere reduced, shorter and narrower than previous segment (Fig. 2E); head with punctures between eyes closer to inner margin of eye; hypomeron not visible in lateral view, without a lobe; mandibles with elongate and thin apical portion, unlike those of *Acylohsellus* (Fig. 2F).
Redefinition. With the removal of *Acylophorus pratensis* from *Acylophorus* (see *Amacylophorus* above), the genus can be defined as having the following phylogenetically important character states: antennae geniculate; first antennomere densely setose; third antennomere densely setose; apical antennomere inflated in narrow profile, shortened and bearing broad microsetose field occupying more than 40% of its length; antennal insertion separated from anterior eye margin by a distance slightly greater than the insertion socket or less, sometimes touching margin; apical labial palpomere reduced, shorter and narrower than previous segment and truncate at apex; proximal tooth of right mandible bifid, trifid or forming a plate (common in Afrotropical fauna); mandibles with apical portion elongate and curved; membranous postcoxal process absent; basisternum without pair of macrosetae; hypomeron not visible in lateral view; scutellum setose; protibia with spines on lateral face; metatibia with at most 2 thin spines on lateral face; protarsomeres cylindrical and without tenent setae ventrally, with pretarsal claws larger than those of mid and hind leg; metatarsomeres elongate, cylindrical and slightly flattened dorsally, segments II–V glabrous dorsally, with empodial setae distinctly longer than those of foreleg; wing veins CuA and MP4 fused; abdominal sternite III with transverse basal line sharply projected at middle; apex of male sternite VIII without emargination; males without external copulatory plate in internal sac of the aedeagus.
Comments. The definition of *Acylophorus* given above encompasses all species that we have been able to examine including those from the Nearctic, Neotropical, Afrotropical, Palaearctic, Oriental and Australian Regions (CNC, cSmet, NHMW). Testing the monophyly of *Acylophorus* was outside of the scope of this study but the genus may be paraphyletic with respect to *Acylohsellus* and *Paratolmerus*. *Acylohsellus* and *Paratolmerus* differ from *Acylophorus* by multiple apomorphies but we have studied several species of *Acylophorus* that suggest the former two genera may be derived from within the latter. The group of species related to *Acylophorus microcephalus* Cameron 1932 from the Himalayas, treated as subgenus *Indoacylophorus* by Bierig (1938), are similar to *Acylohsellus* in body form, maxillary and labial palpi, and the relatively compact mandibles (fig. 24 in Bierig

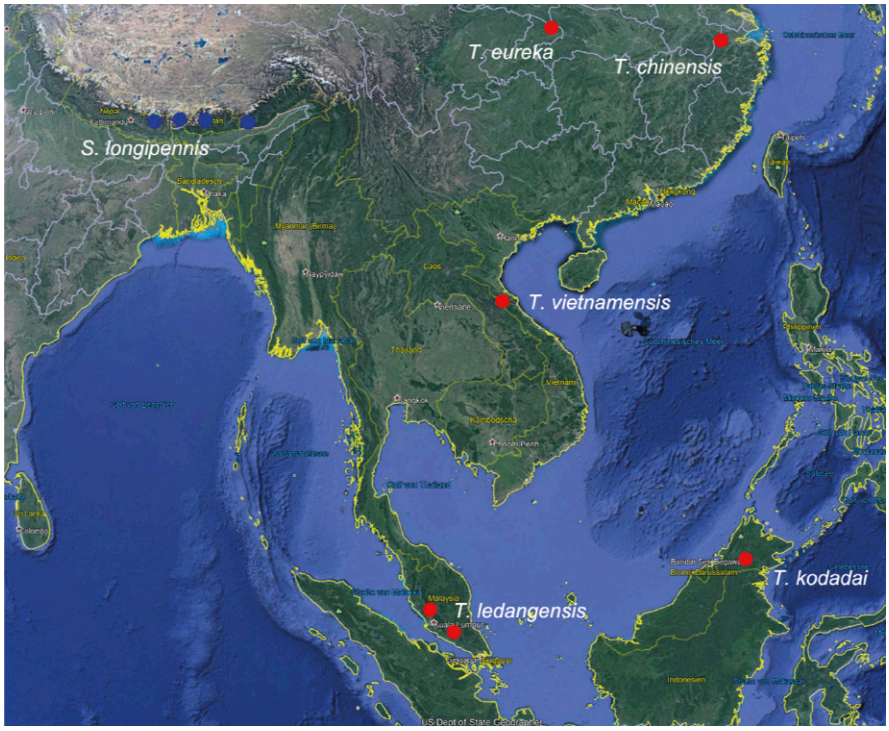

Fig. 7. Distribution of *Stevensia* Cameron (blue) and *Turgiditarsus* Schillhammer (red).

1938). However, they do not have the characteristic male secondary sexual characters, and the extreme modifications of the aedeagus and genital segment, though the median lobe of *A. microcephalus* is similarly shaped (Smetana 1988). The Himalayan species *A. siyo* possesses a pair of long setae on tarsomere 4, a character state otherwise unique to *Paratolmerus* as redefined here. The forebody of this species is also rather convex and the head does have some small groups of setose punctures near the anterior part of the head, indicating a potential relationship to species of *Paratolmerus*. A global-scale phylogenetic analysis of *Acylohsellus*, *Paratolmerus*, and the subgenera and species groups of diverse *Acylophorus* is sorely needed.

4. Discussion

4.1. Higher level phylogeny

In agreement with previous studies (Brunke et al. 2016; Chani-Posse et al. 2018) which overlap in gene sampling, the subtribes of Staphylinini were recovered as monophyletic with high support. Although far outside of the scope of this study, the southern hemisphere lineages formed a well-supported grade as opposed to the unsupported clade in Chani-Posse et al. (2018), with *Afroquedius* resolved as the sister group to all other Staphylinini. The subtribes Amblyopinina, Tanygnathinina and Hyptiomina formed a well-supported clade (ATH clade) that was also recovered by Chani-Posse et al. (2018). *Afroquedius* has been recovered as sister to Amblyopinina in several published phylogenies (Solodovnikov & Schomman 2009; Brunke et al. 2016) but it lacks the fused parameral base and fused wing veins of the ATH clade. A southern hemisphere grade, rather than a clade sister to a northern hemisphere clade, is consistent with the crown and even stem age estimates for Staphylinini in Brunke et al. (2017a), which post-date the break-up of northern Laurasia from southern Gondwana during 170–165 Mya. Under a 'post-break up' origin scenario, Staphylinini would evolve in one of the two land masses and later disperse to the other via land bridges (Eurogondwanan connection of Ezcurra & Agnolín 2012) emergent 145–130 Mya. The topology recovered here supports an origin and early diversification of Staphylinini in Gondwana and later dispersal to Laurasia. However, the taxon sample of the present study is missing some south temperate lineages critical to robust phylogenetic and biogeographic hypotheses, including *Valdiviodes* Smetana, 1981 and recently described *Devilleferus* Jenkins Shaw & Solodovnikov, 2017 (Jenkins Shaw et al. 2017). The position of Australian genus *Antimerus* has never been clearly resolved and although it was recovered by the present analysis as the sister group of the northern hemisphere clade with high support, this hypothesis should be tested with greater taxon sampling. The backbone topology within the northern hemisphere clade of Brunke et al. (2016), recovered with molecular data only, is corroborated here with a total evidence dataset (Fig. 3). The sister group relationship between Erichsoniina and Acylophorina, hypothesized by Brunke et al. (2016) but unresolved in Chani-Posse et al. (2018) with limited taxon sampling of Acylophorina, was recovered with high support in our analysis, which included a novel shared character on the apical antennomere (see Results, Taxonomy).

4.2. Evolution of Acylophorina and placement of *Turgiditarsus*

Turgiditarsus was recovered within a monophyletic Acylophorina with high support, far outside of the Anisolinina where it was previously classified. The Oriental genus was resolved with high support as the sister group to the eastern North American *Hemiquedius*. Although the two genera are rather different in habitus, they do share a spine-less foretibia and a similarly shaped and punctate head (Fig. 4). All genera proposed by Brunke et al. (2016) to belong to Acylophorina, including *Stevensia*, were recovered within this clade in the present study. The elongate, more cylindrical pronotum (not coded in matrix) shared between the earliest diverging lineages of Acylophorina (*Hemiquedius*, *Stevensia*, *Turgiditarsus*) and *Erichsonius* (Erichsoniina) (Figs. 3, 4) suggests that this pronotum shape evolved in the common ancestor of these two subtribes and independently in the common ancestor of Staphylinini Propria (Fig. 3). The pronotum appears to have reversed to the '*Quedius*-like', shield shape in the common ancestor of *Anaquedius* and its sister clade (Figs. 3, 4). The unintuitive evolution of pronotum morphology and its associated morphological characters within the Erichsoniina-Acylophorina lineage has previously led to inaccurate morphology-based phylogenies and un-natural systematics (e.g. *Erichsonius* as Staphylinini Propria in Solodovnikov et al. 2013 and Brunke & Solodovnikov 2013). As a consequence, *Stevensia*, *Turgiditarsus* and *Erichsonius* have been associated with the Staphylinini Propria clade at some point in history.

Despite sharing conspicuously glabrous elytra and a distribution in eastern North America, *Hemiquedius* and *Anaquedius* are not each other's closest living relatives (Fig. 4); this corroborates the topology found by Brunke et al. (2016) using molecular data alone. Recent phylogenies resolving these two genera as sister taxa (Chani-Posse et al. 2018; Żyła & Solodovnikov 2017) have either included no other Acylophorina (former) or did not include *Stevensia* or *Turgiditarsus* in their taxon sample (latter). The closer relationship of *Anaquedius* to *Australotarsius* and the *Acylophorus* lineage than to *Hemiquedius* is supported by several morphological characters given in Fig. 4. The unique external copulatory plate of the aedeagus (Fig. 6), found in many early diverging Acylophorina, is likely to be a synapomorphy of the subtribe that was later lost in the common ancestor of clade 4 (Fig. 4). Although previously cited as a possible characteristic of the entire subtribe (Solodovnikov & Schomann 2009; Solodovnikov & Newton 2009), the non-emarginate male sternite VIII likely evolved much later, in the common ancestor of clade 3 (Fig. 4).

The *Acylophorus* lineage, defined herein (see Taxonomy, clade 5 in Fig. 4) was resolved as a well-supported clade with multiple morphological synapomorphies, congruent with previous phylogenies despite their wide range in taxon sampling (Chatzimanolis et al. 2010; Brunke et al. 2016; Jenkins Shaw et al. 2017; Żyła & Solodovnikov 2017). This group is the most diverse lineage within the subtribe with over 165 species and is most easily recognized by the geniculate antennae. The only known fossil Acylophorina, from Baltic amber, was recently described and placed in this lineage as *Acylophorus hoffeinsorum* Żyła & Solodovnikov, 2017. Based on the new morphological concepts of genera given herein (Taxonomy), the generic assignment of this fossil may need to be re-evaluated in the future, as the authors mentioned similarities to *Amacylophorus*. Although it was possible to morphologically diagnose the genera of the *Acylophorus* lineage (see Taxonomy), it was outside of the scope of this study to test the monophyly of *Acylophorus*, with respect to *Paratolmerus* and *Acylohsellus*. It is possible that these genera may be nested inside of *Acylophorus* based on a preliminary morphological survey (see Taxonomy). Few species of *Acylophorus* have been included in phylogenetic analyses and a dedicated effort to sample the many species groups and subgenera of the genus will be necessary to delineate monophyletic groups in this complex.

4.3. Relictualism in ancient Acylophorina

With the exception of clade 6 in Fig. 4, most acylophorine genera are strikingly species poor, morphologically disparate and restricted to a specific biogeographic region or subregion (Fig. 4). Most of these genera are very rarely collected, suggesting a narrow range of microhabitats or generally smaller populations in the larger environment. These qualities are predicted for older lineages in the final stage of the 'taxon cycle', which have experienced greater extinction than younger groups and have contracted, or relictual, ranges (Jønsson et al. 2017). Divergence date estimates from Brunke et al. (2017a) suggest a Laurasian origin for crown Acylophorina in the latest Early Cretaceous (107.6 Mya) and an earliest Late Cretaceous (96.6 Mya) age of the common ancestor of *Anaquedius* and the *Acylophorus* lineage (minus *Amacylophorus*) (see Fig. 4 for topology). The ages of these earlier diverging lineages (107–96 Mya), now restricted to either eastern North America or Asia, are coincident with the North American intercontinental seaway, which divided the continent into eastern and western halves from 100–84 Mya and prevented dispersal between eastern North America and Asia (via western North America); dispersal was also not yet possible to Asia via Europe (Sanmartín et al. 2001). Much later, during the early Cenozoic, land bridges permitted dispersal of vertebrates, plants and insects between eastern North America, Europe, and Asia (Brikiatus 2014; Chin et al. 2014; Brunke et al. 2017a). Therefore, the direct common ancestor of *Turgiditarsus* and *Hemiquedius*, and ancestors of *Anaquedius*, *Amacylophorus* and *Stevensia* (Fig. 4) must have been more widely distributed in the early Cenozoic, including Europe, and may eventually be discovered in Eocene fossils such as European Baltic Amber. Without more detailed divergence dating

of a more inclusive taxon sample or the discovery of additional fossils, it is not possible to determine whether diversification into extant genera occurred in the Cretaceous or later, in the Eocene.

The *Acylophorus* lineage (minus *Amacylophorus*) is apparently much younger, with an estimated early Palaeocene age (63.4 Mya) (Brunke et al. 2017a). This clade is notable for its occurrence in all major biogeographic regions and on islands such as Madagascar, Sri Lanka, Cuba, Hispaniola, the Philippines and New Guinea. These characteristics suggest that the *Acylophorus* lineage (minus *Amacylophorus*) is in the earlier stages of the taxon cycle, with a relatively large number of species, broad distribution and apparently high dispersal capacity (Jønsson et al. 2017). At least 3 dispersals from the Oriental region to the Australian Region have taken place in the Acylophorina (*Acylophorus*, *Anchocerus*, *Australotarsius*, and possibly *Acylohsellus*) (Solodovnikov 2008; Solodovnikov & Newton 2009), likely across island chains – first during the mid-Miocene and later to Australia in the late Miocene (Hall 2013). While many species of *Acylophorus* and *Anchocerus* are known from southeast Asia, *Australotarsius* is still only known from few specimens from eastern Australia and Tasmania (Solodovnikov & Newton 2009), and may yet be discovered in New Guinea, Wallacea or Sundaland.

Although the 95% probability distributions for the age estimates in Acylophorina were the widest of any subtribe in Brunke et al. (2017a), they are the only divergence dates available for this lineage thus far. These large confidence intervals were likely due to a lack of reliably identified fossils of Acylophorina available for calibration at that time (but see Żyła & Solodovnikov 2017). Greater confidence in the scenarios proposed here will require dating studies with a greater range of taxon sampling for the group (elucidated here) and the addition of newly available fossils for calibration.

5. Conclusions

Despite its highly divergent morphology, *Turgiditarsus* was confidently resolved as a member of the Acylophorina using a combination of morphological and molecular data. The phylogenetic hypothesis for the subtribe presented herein is most taxonomically comprehensive to date and is well resolved, though much remains to be understood in the diverse *Acylophorus* lineage. Future taxonomic and phylogenetic research should focus on a more comprehensive taxon sampling of this clade at a global scale. The results of our phylogenetic analysis confirm previous systematic and phylogenetic hypotheses, which demonstrate that pronotum shape has misled the classification of several Acylophorina and their relatives. The ancient Cretaceous origins of the subtribe and its earlier diverging lineages, as indicated by recent divergence dating (Brunke et al. 2017a), are consistent with the restricted distribution, isolated phylogenetic position and low diversity of most genera. Eastern North American wetlands, mountain valleys of the Himalayas, and lowland southeast Asian forests have acted as important refugial areas for lineages which were once widespread across the northern hemisphere. The converse appears to be the case for the much younger *Acylophorus* lineage, especially *Acylophorus*, which occurs in all major biogeographic regions. However, some genera are so rarely collected (*Turgiditarsus*, *Australotarsius*, *Stevensia*) that they may eventually be discovered in other regions or additional new genera may still be undiscovered. It is our hope that the comprehensive identification key and improved diagnoses of such rare genera will encourage their discovery both in the field and in museum collections. In fact, it was a single old specimen of *Turgiditarsus* discovered in the Smithsonian, which prompted this entire study.

6. Acknowledgements

The help of colleagues listed in the methods section is greatly appreciated. A. Smetana (Ottawa, Canada) provided some additional specimens of *Paratolmerus*, *Acylohsellus* and *Anchocerus* for study and was available for many productive discussions on morphological characters. We thank K.V. Makarov (www.zin.ru/animalia/coleoptera) for the use of their photograph of *Acylophorus wagenschieberi*. V. Grebennikov (Ottawa, Canada) kindly provided his light source/diffuser system for specimen photography.

7. References

Bierig A. 1938. Sobre el genero *Acylophorus* (Col. Staph), division subgenerica y descripcion de nuevas especies neotropicales. – Memorias de la Sociedad Cubana de Historia Natural **12**: 119–138.

Bouchard P., Bousquet Y., Davies A., Alonso-Zarazaga M.A., Lawrence J.F., Lyal C.H.C., Newton A.F., Reid C.A.M., Schmitt M., Slipinski S.A., Smith A.B.T. 2011. Family-Group Names in Coleoptera (Insecta). – ZooKeys **88**: 1–972.

Brunke A., Solodovnikov A. 2013. *Alesiella* gen.n. and a newly discovered relict lineage of Staphylinini (Coleoptera: Staphylinidae). – Systematic Entomology **38**: 689–707.

Brunke A., Solodovnikov A. 2014. A revision of the Neotropical species of *Bolitogyrus* Chevrolat, a geographically disjunct lineage of Staphylinini (Coleoptera, Staphylinidae). – ZooKeys **423**: 1–113.

Brunke A.J., Chatzimanolis S., Schillhammer H., Solodovnikov A. 2016. Early evolution of the hyperdiverse rove beetle tribe Staphylinini (Coleoptera: Staphylinidae: Staphylininae) and a revision of its higher classification. – Cladistics **32**: 427–451.

Brunke A., Chatzimanolis S., Metscher B.D., Wolf-Schwenninger K., Solodovnikov A. 2017a. Dispersal of thermophilic beetles across the intercontinental Arctic forest belt during the early Eocene. – Scientific Reports **7**: 12972.

Brunke A., Smetana A., Carruthers-Lay D., Buffam J. 2017b. Revision of *Hemiquedius* Casey (Staphylinidae, Staphylininae) and a review of beetles dependent on beavers and muskrats in North America. – ZooKeys **702**: 27–43.

Cameron M. 1932. The fauna of British India including Ceylon and Burma. Coleoptera. Staphylinidae. – London, Talyor and Francis. xii + 1–443.

Chani-Posse M., Brunke A., Chatzimanolis S., Schillhammer H., Solodovnikov A. 2018. Phylogeny of the hyper-diverse rove beetle subtribe Philonthina with implications for classification of the tribe Staphylinini (Coleoptera: Staphylinidae). – Cladistics **34**: 1–40.

Chatzimanolis S., Cohen I.M., Schomann A.S., Solodovnikov A. 2010. Molecular phylogeny of the mega-diverse rove beetle tribe Staphylinini (Insecta, Coleoptera, Staphylinidae). – Zoologica Scripta **39**: 436–449.

Chin S.-W., Shaw J., Haberle R., Wen J., Potter D. 2014. Diversification of almonds, peaches, plums and cherries – molecular systematics and biogeographic history of *Prunus*. – Molecular Phylogenetics and Evolution **76**: 34–48.

Ezcurra M.D., Agnolín F.L. 2012. A new global palaeobiogeographical model for the Late Mesozoic and Early Tertiary. – Systematic Biology **61**: 553–566.

Fauvel A. 1905. Staphylinides exotiques nouveaux (3e partie). – Revue d'Entomologie **24**: 113–147

Hall R. 2013. Sundaland and Wallacea: geology, plate tectonics and palaeogeography. Pp. 32–78 in: Gower D., Johnson K., Richardson J.E., Rosen B., Rüber L., Williams S. (eds), Biotic evolution and environmental change in southeast Asia – Cambridge University Press, Cambridge, United Kingdom. 496 pp.

Herman L. 2001. Nomenclatural changes in the Staphylinidae (Insecta: Coleoptera). – Bulletin of the American Museum of Natural History No. **264**: 83 pp.

Hu J.-Y., Li L.-Z., Zhao M.-J. 2012. Three new species of *Anchocerus* Fauvel (Coleoptera: Staphylinidae: Staphylininae), with an updated key to Chinese species. – Zootaxa **3318**: 57–62.

Janak J. 2017. Four new species and a new record of *Anchocerus* from the Oriental region (Coleoptera: Staphylinidae: Staphylininae: Staphylinini: Acylophorina). – Zootaxa **4319**: 579–589.

Jenkins Shaw J., Żyła D., Solodovnikov A. 2017. A spectacular new genus of Staphylinini rove beetle from the tropical Andes and its phylogenetic assessment (Coleoptera: Staphylinidae). – Invertebrate Systematics **31**: 713–722.

Jønsson K.A., Borregaard M.K., Carstensen D.W., Hansen L.A., Kennedy J.D., Machac A., Marki P.Z., Fjeldså J., Rahbek C. 2017. Biogeography and biotic assembly of Indo-Pacific corvoid passerine birds. – Annual Review of Ecology, Evolution and Systematics **48**: 231–253.

Katoh K., Misawa K., Kuma K., Miyata T. 2002. MAFFT: a novel method for rapid multiple sequence alignment based on fast Fourier transform. – Nucleic Acids Research **30**: 3059–3066.

Kypke J.L., Solodovnikov A., Brunke A., Yamamoto S., Żyła D. in press. The past & the present through phylogenetic analysis: the rove beetle tribe Othiini now and 99 million years ago. – Systematic Entomology.

Lanfear R., Calcott B., Ho S., Guindon S. 2012. PartitionFinder: combined selection of partitioning schemes and substitution models for phylogenetic analyses. – Molecular Biology and Evolution **29**: 1695–1701.

Lott D. 2010. The species of *Acylophorus* Nordmann (Coleoptera: Staphylinidae: Staphylininae) in continental sub-Saharan Africa. – Zootaxa **2402**: 1–51.

Maddison W.P., Maddison D.R. 2017. Mesquite: a modular system for evolutionary analysis. v3.3. – Available from <http://mesquiteproject.org>.

Nordmann A. 1837. Symbolae ad monographiam staphylinorum. Ex Academiae Caesareae Scientiarum. – Petropoli, Academiae Caesareae Scientiarum. 1–167.

Outerelo R., Gamarra P. 1985. 10. Las familias y géneros de los estafilínidos de la Península Ibérica. Claves para la identificación de la fauna Española. – Madrid, Universidad Complutense. 139.

Rambaut A., Suchard M., Xie D., Drummond A. 2014. Tracer v1.6. – Available from <http://beast.bio.ed.ac.uk/Tracer>.

Reichle D.E. 1966. Some pselaphid beetles with boreal affinities and their distribution along the Postglacial Fringe. – Systematic Zoology **15**: 330–344.

Ronquist F., Teslenko M., Van Der Mark P., Ayres D., Darling A., Höhna S., Larget B., Liu L., Suchard M., Huelsenbeck J. 2012. MrBayes 3.2: efficient Bayesian phylogenetic inference and model choice across a large model space. – Systematic Biology **61**: 539–542.

Rougemont G. 1991. A second species of *Paratolmerus* Cameron (Col., Staphylinidae, Quediinae). – Entomologist's Monthly Magazine **127**: 221–223.

Schillhammer H. 1996. New genera and species of Asian Staphylinini. – Koleopterologische Rundschau **66**: 59–71.

Schillhammer H. 1997. *Turgiditarsus*, a new name for *Tumiditarsus* Schillhammer with a description of a new species (Coleoptera: Staphylinidae). – Entomological Problems **28**: 109–110.

Schillhammer H. 2004. Critical notes on the subtribe Anisolinina with descriptions of nine new species (Coleoptera: Staphylinidae: Staphylininae). – Koleopterologische Rundschau **74**: 251–277.

Schillhammer H. 2011. Old and new Staphylinini from the Palearctic and Oriental regions. – Koleopterologische Rundschau **81**: 133–163.

Schülke M., Smetana A. 2015. Staphylinidae. Pp. 901–1134 in: I. Löbl, D. Löbl (eds), Catalogue of Palaearctic Coleoptera. – Brill, Leiden, The Netherlands. 1702 pp.

Smetana A. 1971. Revision of the tribe Quediini of North America north of Mexico (Coleoptera: Staphylinidae). – Memoirs of the Entomological Society of Canada No. **79**: 1–303.

Smetana A. 1981. Revision of the tribe Quediini of America North of Mexico (Coleoptera: Staphylinidae). Supplementum 5. – The Canadian Entomologist **113**: 631–644.

Smetana A. 1988. Revision of the tribes Quediini and Atanygnathinini. Part II. The Himalayan region (Coleoptera: Staphylinidae). – Quaestiones Entomologicae **24**: 163–464.

Smetana A. 1995a. *Acylohsellus*, a new genus for *Acylophorus longiceps* Cameron, 1918 (Coleoptera: Staphylinini: Quediina). – Entomologische Blätter **91**: 113–118.

Smetana A. 1995b. Revision of the tribes Quediini and Tanygnathinini. Part III. Taiwan. (Coleoptera: Staphylinidae). – National Museum of Natural Science – Special Publication No. **6**. 145 pp.

Smetana A. 2018. Taxonomic review of the 'quediine' subtribes of Staphylinini of mainland China (Coleoptera: Staphylinidae: Staphylininae). – Prague, Jan Farkač. 400 pp.

Smetana A., Davies A. 2000. Reclassification of the north temperate taxa associated with *Staphylinus* sensu lato, including comments on relevant subtribes of Staphylinini (Coleoptera: Staphylinidae). – American Museum Novitates **3287**: 1–88.

Solodovnikov A.Y. 2006. Revision and phylogenetic assessment of *Afroquedius* gen. nov. from South Africa: toward new concepts of the genus *Quedius*, subtribe Quediina and reclassification of the tribe Staphylinini (Coleoptera: Staphylinidae: Staphylininae). – Annals of the Entomological Society of America **99**: 1065–1084.

Solodovnikov A. 2008. Review of the Oriental genus *Anchocerus* with the description of new species and new combinations (Coleoptera: Staphylinidae: Staphylininae). – Insect Systematics and Evolution **39**: 287–301.

Solodovnikov A., Newton A. 2009. *Australotarsius* – a new genus of the rove beetle tribe Staphylinini from Australia (Coleoptera: Staphylinidae: Staphylininae). – Zootaxa **2033**: 49–57.

Solodovnikov A., Schomann A. 2009. Revised systematics and biogeography of 'Quediina' of sub-Saharan Africa: new phylogenetic insights into the rove beetle tribe Staphylinini (Coleoptera: Staphylinidae). – Systematic Entomology **34**: 443–466

Solodovnikov A., Yue Y., Tarasov S., Ren D. 2013. Extinct and extant rove beetles meet in the matrix: Early Cretaceous fossils shed light on the evolution of a hyperdiverse insect lineage (Co-

leoptera: Staphylinidae: Staphylininae). – Cladistics **29**: 360–403.

Talavera G., Castresana J. 2007. Improvement of phylogenies after removing divergent and ambiguously aligned blocks from protein sequence alignments. – Systematic Biology **56**: 564–577.

Webster R., Smetana A., Sweeney J., Demerchant I. 2012. New Staphylinidae (Coleoptera) records with new collection data from New Brunswick and an addition to the fauna of Quebec: Staphylininae. – ZooKeys **186**: 293–348.

Żyła D., Solodovnikov A. 2017. First extinct representative of the rove beetle subtribe Acylophorina from Baltic amber and its phylogenetic placement. – Journal of Systematic Paleontology. doi: 10.1080/14772019.2017.1399171.

Electronic Supplement File

at http://www.senckenberg.de/arthropod-systematics

File 1: schillhammer&brunke-staphylinidaeturgiditarsus-asp2018-electronicsupplement.docx — **Table S1.** Specimens and GenBank accession numbers for taxa used in phylogenetic analyses of molecular data. Missing data are indicated with a dash (–).

Zoobank Registrations

at http://zoobank.org

Present article: urn:lsid:zoobank.org:pub:EE63DA0A-CFF5-4903-82E6-B3C798EFACFE

***Turgiditarsus eureka* Schillhammer & Brunke, 2018:** urn:lsid:zoobank.org:act:C16E2968-2E20-469B-A23C-4851247A8884

***Turgiditarsus vietnamensis* Schillhammer & Brunke, 2018:** urn:lsid:zoobank.org:act:152362DC-24BB-4451-819D-6AF39E943F78